Pore condensation and freezing: Close up on how porous particles nucleate ice

Claudia Marcolli

ETH Zürich

Pore condensation and freezing (PCF)

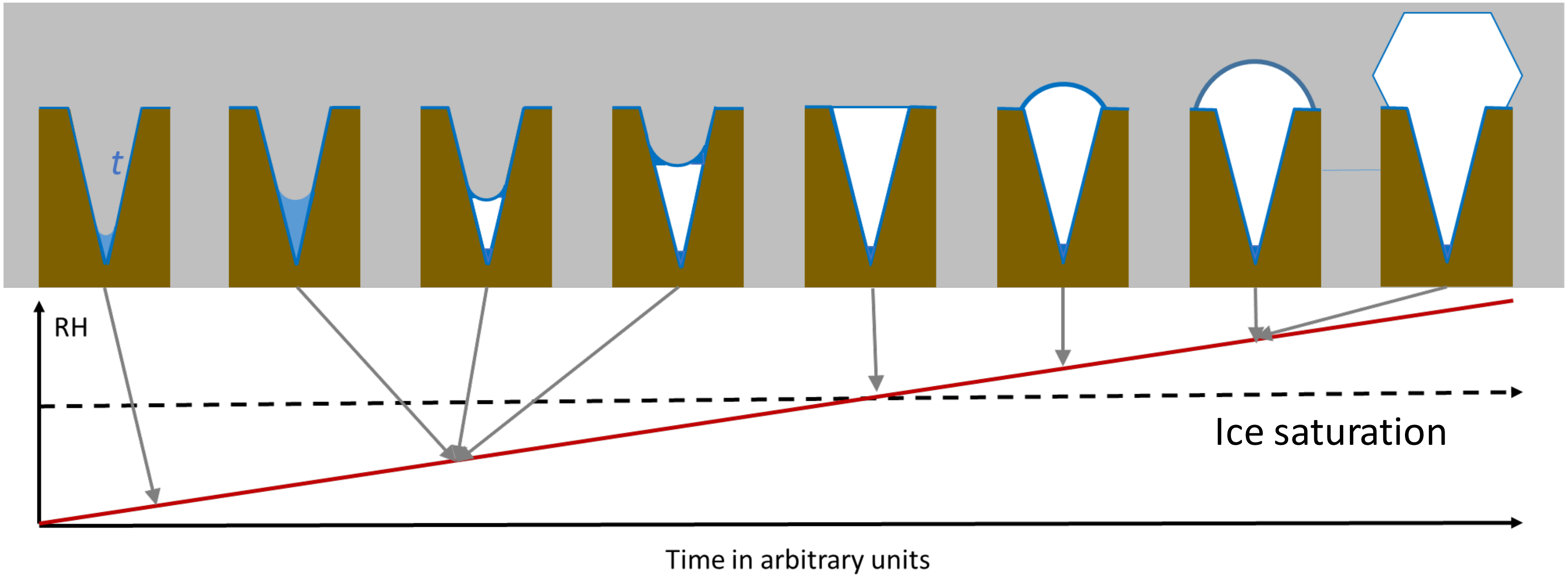

Fukuta, JAS, 1966: PCF used to explain pre-activation

Activation of Atmospheric Particles as Ice Nuclei in Cold and Dry Air

ABSTRACT

Ice nucleation and subsequent phase equilibrium in water held in the micro-capillaries of atmospheric particles are examined. It is found that ice formed in the micro-capillaries of certain particles may exist in equilibrium with a dry atmosphere, where particles preactivated by Fournier's effect are expected to lose their activity. A possible mechanism of activation of the particles as ice nuclei in a cold dry atmosphere is suggested.

2. Condensation of water vapor in a micro-capillary
3. Nulceation of ice in capillary-held water
4. Freezing and melting of ice in capillary-held water
5. Sublimation and deposition of ice in a capillary system
6. Effect of a soluble impurity on the melting point of capillary ice
7. Experimental evidence of phase changes of capillary-held water

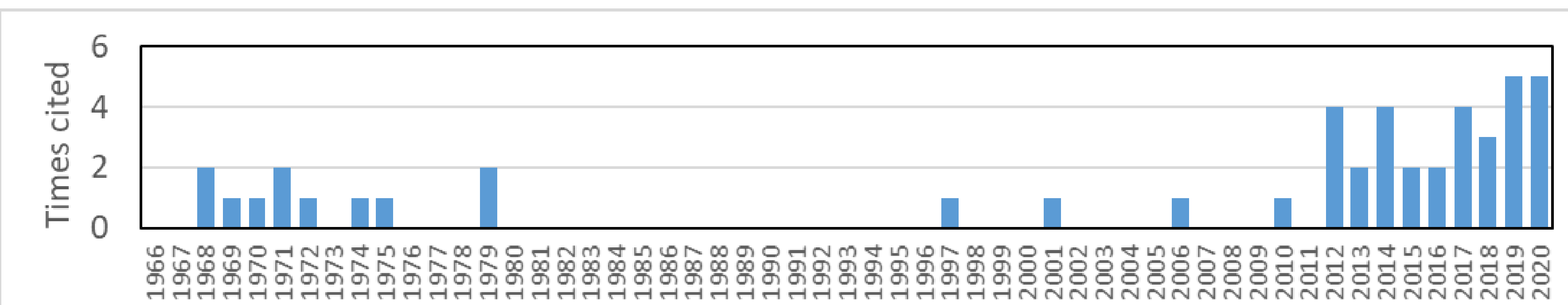

Fukuta, JAS, 1966: PCF used to explain pre-activation

Activation of Atmospheric Particles as Ice Nuclei in Cold and Dry Air

ABSTRACT

Ice nucleation and subsequent phase equilibrium in water held in the micro-capillaries of atmospheric particles are examined. It is found that ice formed in the micro-capillaries of certain particles may exist in equilibrium with a dry atmosphere, where particles preactivated by Fournier's effect are expected to lose their activity. A possible mechanism of activation of the particles as ice nuclei in a cold dry atmosphere is suggested.

2. Condensation of water vapor in a micro-capillary
3. Nulceation of ice in capillary-held water
4. Freezing and melting of ice in capillary-held water
5. Sublimation and deposition of ice in a capillary system
6. Effect of a soluble impurity on the melting point of capillary ice
7. Experimental evidence of phase changes of capillary-held water

«Thus, the results of various observations of phase change in capillary-held water and the present theoretical study support the possibility of phase transition of sorbed water in the capillaries of an atmospheric particle which will later be the center of ice crystal growth.»

What evidence is required for PCF

- Increase in activated fraction when temperature falls below the homogeneous ice nucleation threshold
- Presence of pores in ice-nucleating particles
- Pore condensation occurring well below water saturation
- Ability of ice to nucleate within very small water volumes
- Ability of ice to grow out of the pores from the vapor phase

Acknowledgments

Thomas Peter
Beiping Luo
Ulrike Lohmann
Zamin Kanji
Rob David
Jonas Fahrni
Yuqing Qiu
Yamila Perez Sirkin
Valeria Molinero
Fabian Mahrt
Dominik Brühwiler
Philipp Grönquist
Eszter Barthazy Meier
Kevin Kilchhofer
Michael Rösch
Bernd Kärcher

What evidence is required for PCF

- Increase in activated fraction when temperature falls below the homogeneous ice nucleation threshold
- Presence of pores in ice-nucleating particles
- Pore condensation occurring well below water saturation
- Ability of ice to nucleate within very small water volumes
- Ability of ice to grow out of the pores from the vapor phase

Freezing onsets of kaolinite particles

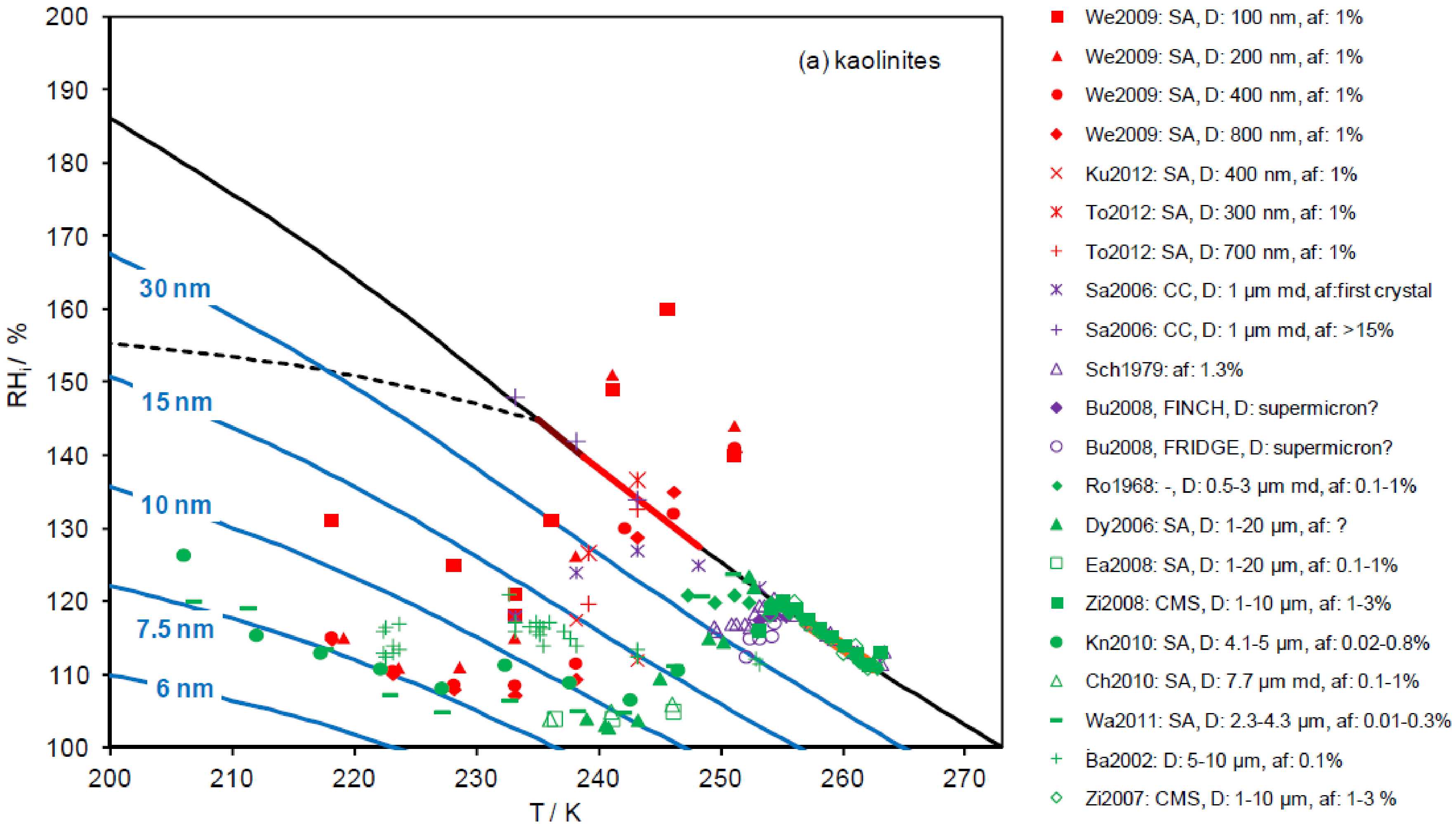

Marcolli, 2014

Kaolinite: From deposition nucleation to condensation freezing

Zurich Ice Nucleation Chamber ZINC

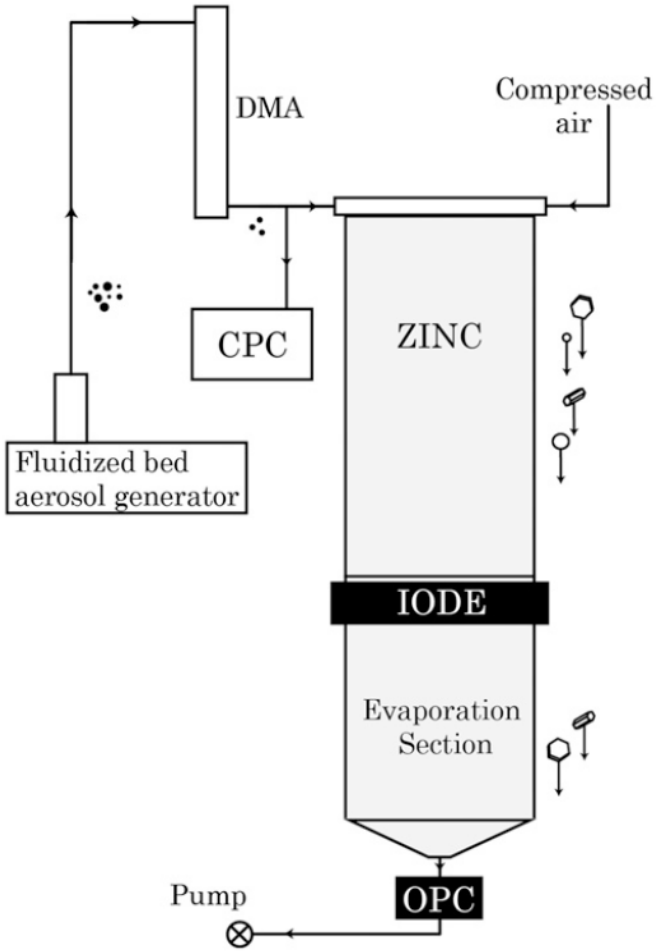

Activated fraction as a function of Rh_i

Kaolinite (Fluka)

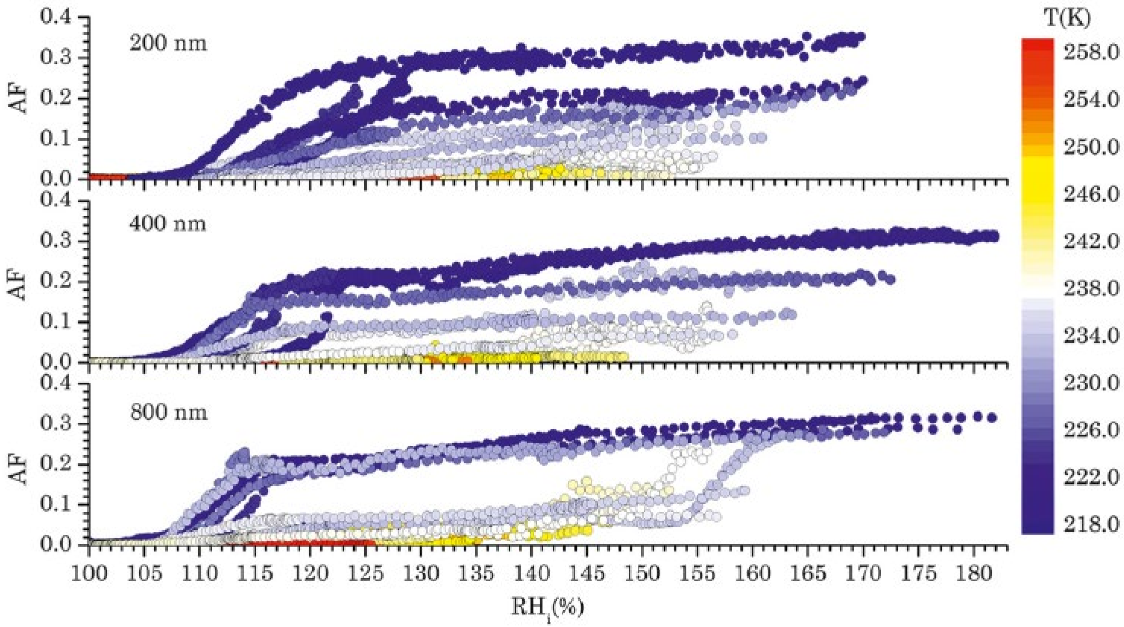

Welti et al., 2014

Activated fraction of kaolinite particles: contour diagrams

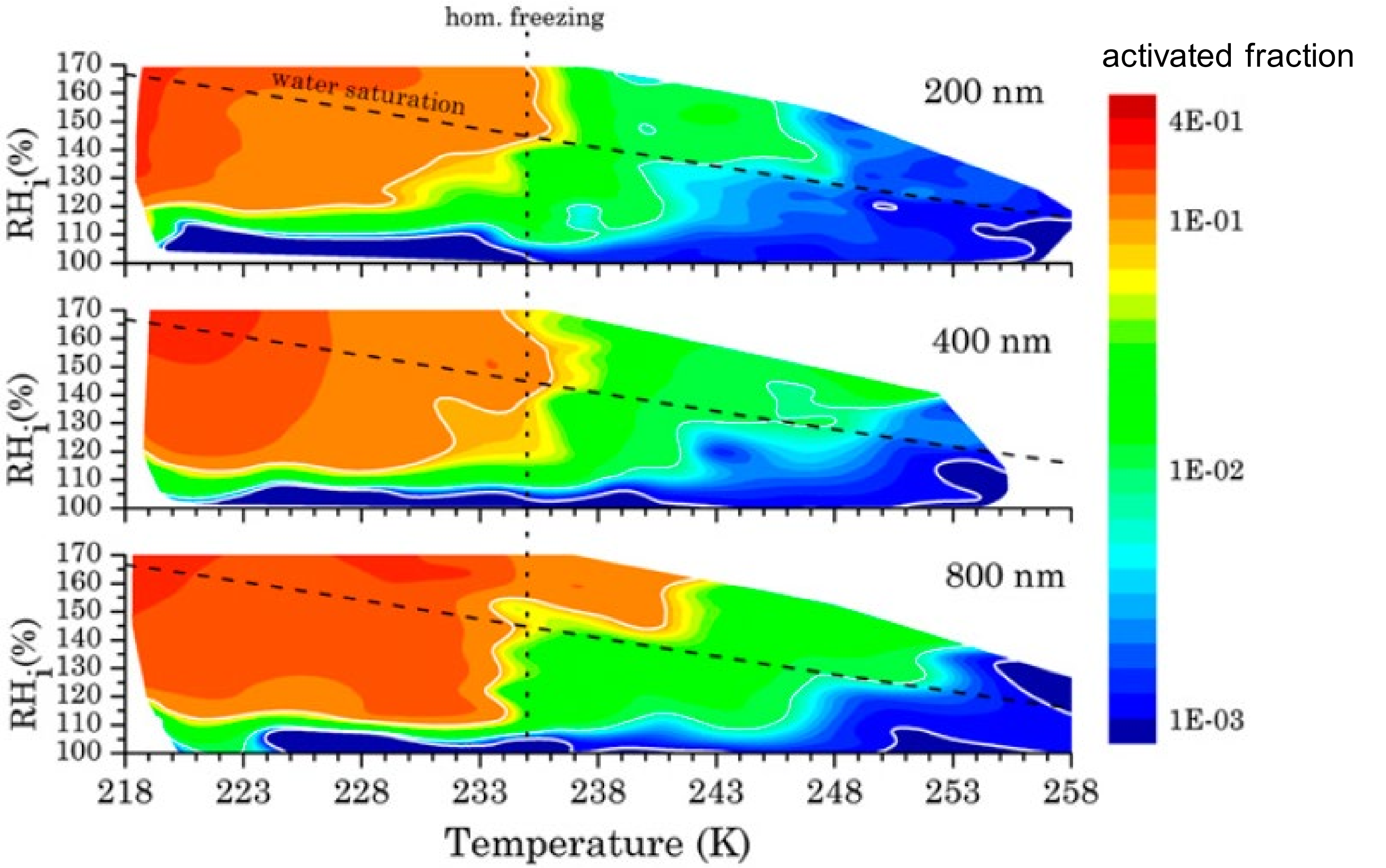

Welti et al., 2014

Modeling of experimental results using CNT and assuming a deposition nucleation process

One constant contact angle | Probability density function of contact angles

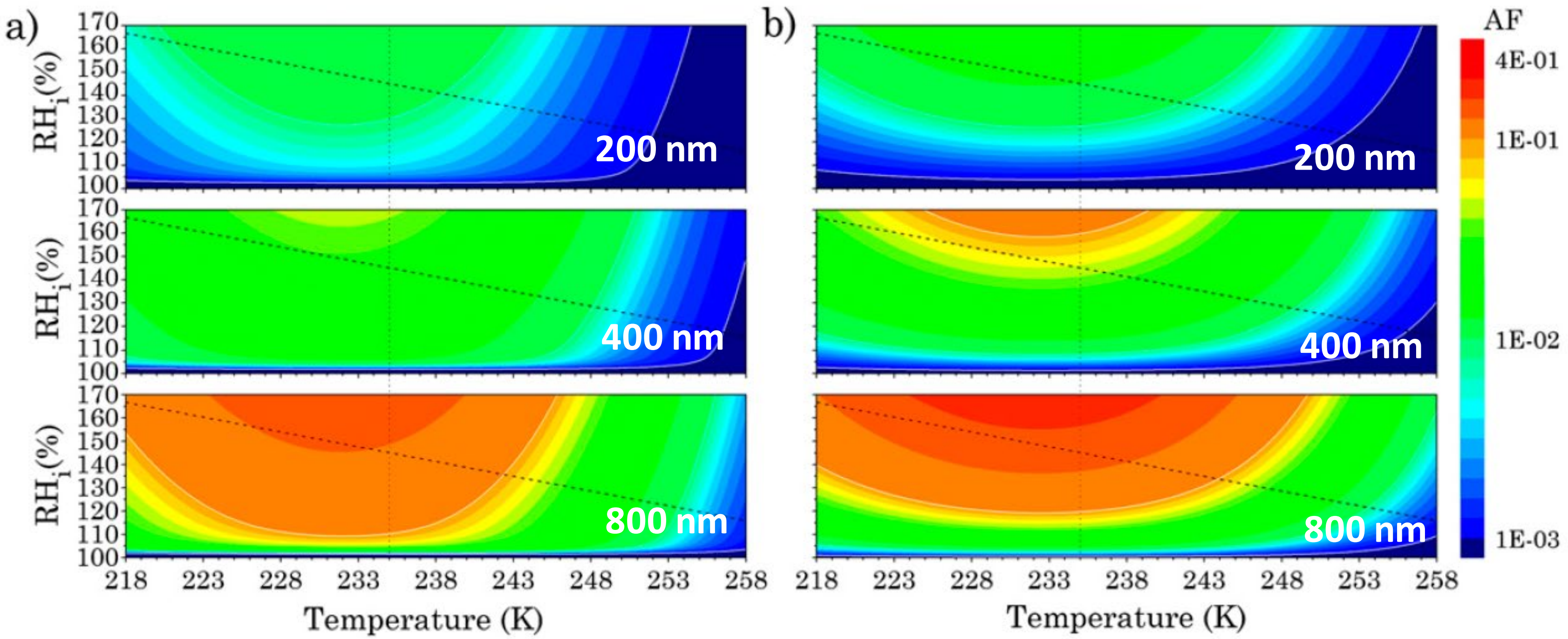

« Abstract: …The observed increase in the activated fraction below water saturation and temperatures below 235 K corroborate the assumption that an appreciable amount of adsorbed or capillary condensed water is present on kaolinite particles, which favors ice nucleation.»

Welti et al., 2014

Kaolinite

Clay mineral ($Al_4[(OH)_8|Si_4O_{10}]$)

Stacking of lamellae leads to platy particles with pores resulting from the interleaving of the plates.
Typical pore diameters: 20 – 50 nm

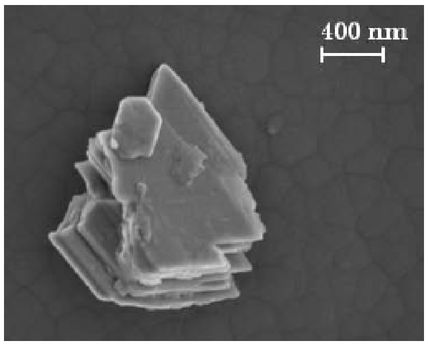

Kaolinite (Fluka)
SEM images
(Welti et al., 2009):

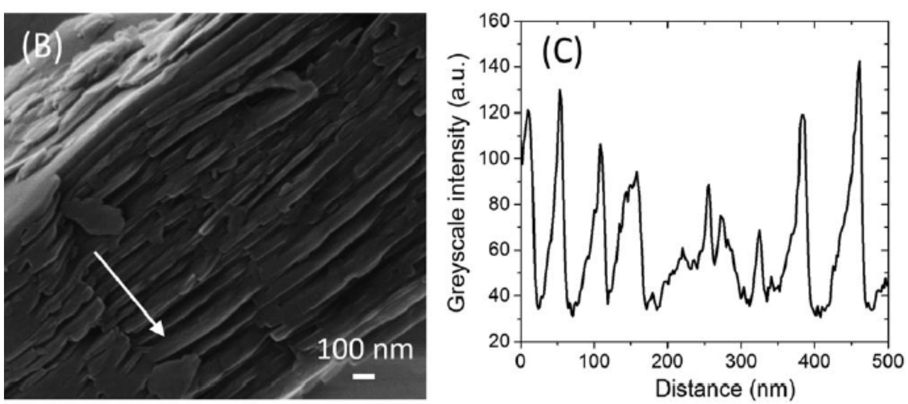

HeIM images (Wang et al., 2016)

Immersion freezing

Differential scanning calorimetry

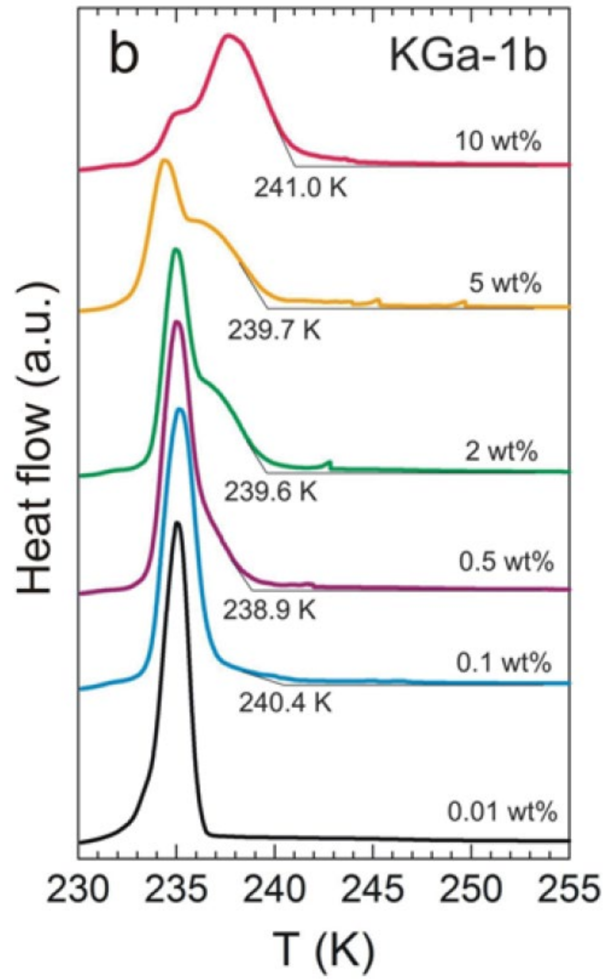

Pinti et al., 2012

Mesoporous silica materials

MCM-41
Cylindrical pores:
2 – 5 nm

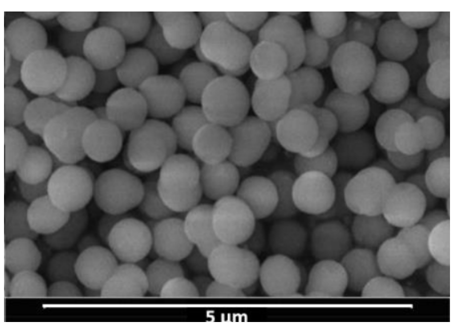

SBA-15
Cylindrical pores:
4 – 20 nm

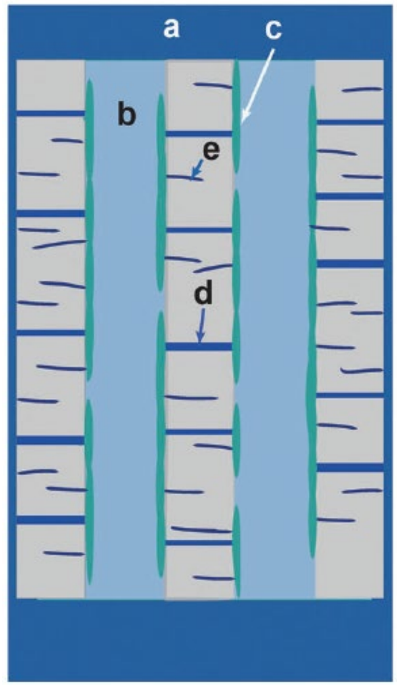

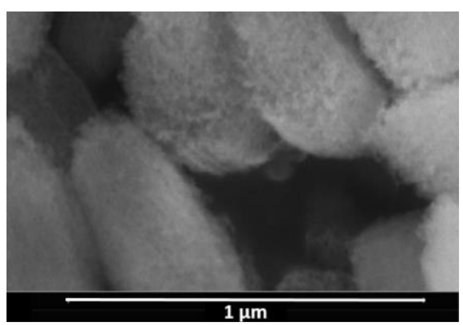

SBA-16
Cages:
6 – 11 nm

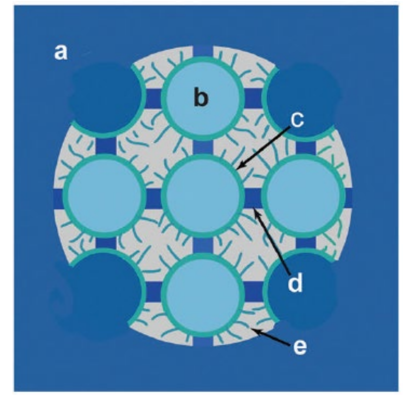

(a) external bulk-like water
(b) water in main pores
(c) boundary water
(d) water in the inter-connecting cylindrical pores
(e) water in the micropores or coronas.

→amorphous pore walls
→ Si-O-Si backbone

Kittaka et al., 2011

ZINC (Zurich Ice Nucleation Chamber) with mesoporous silica particles

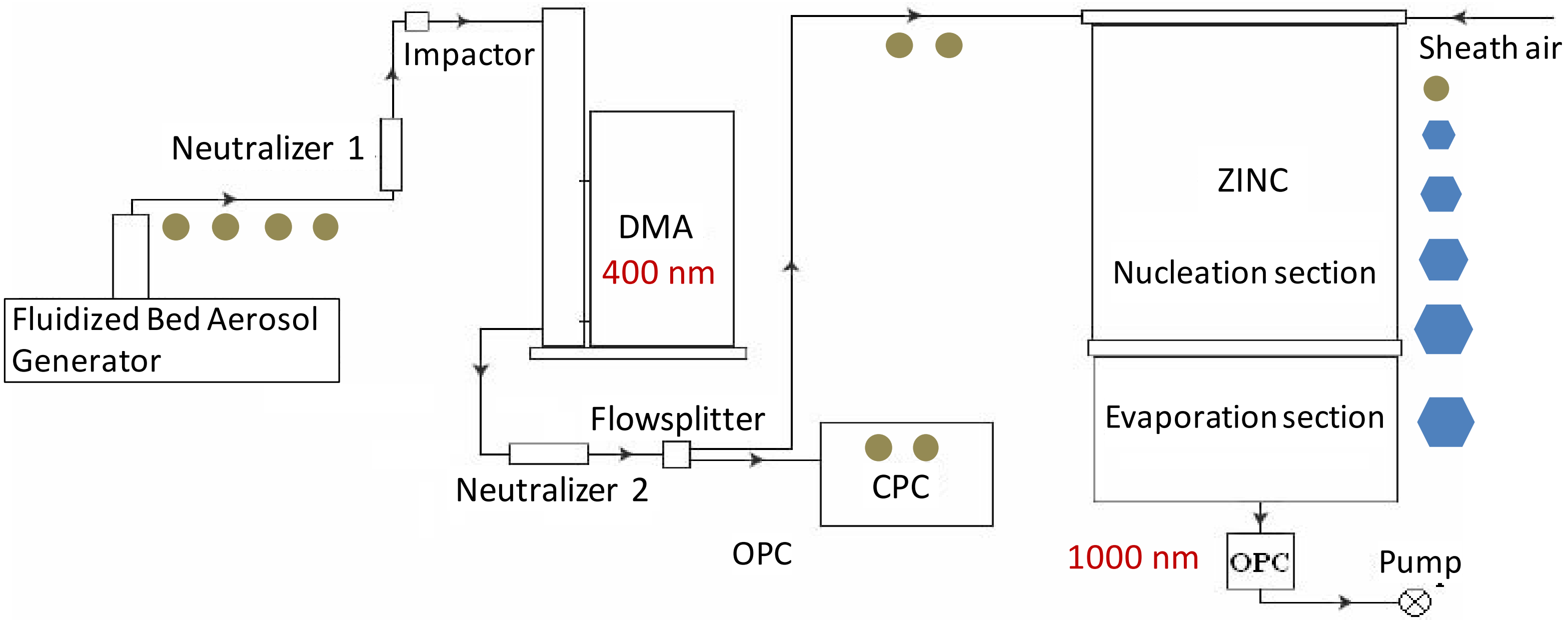

MCM-41

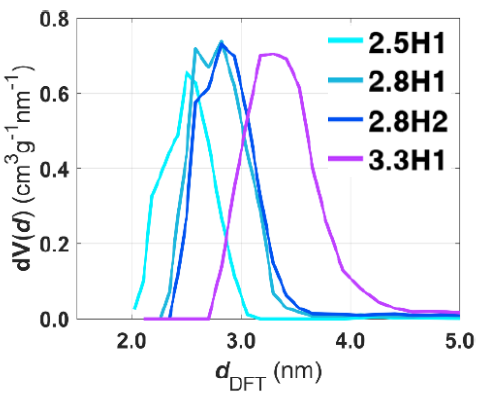

SBA-15

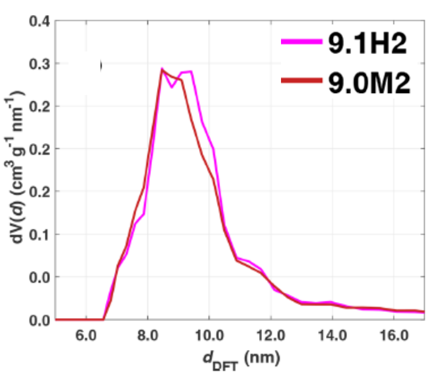

David et al., 2019, 2020

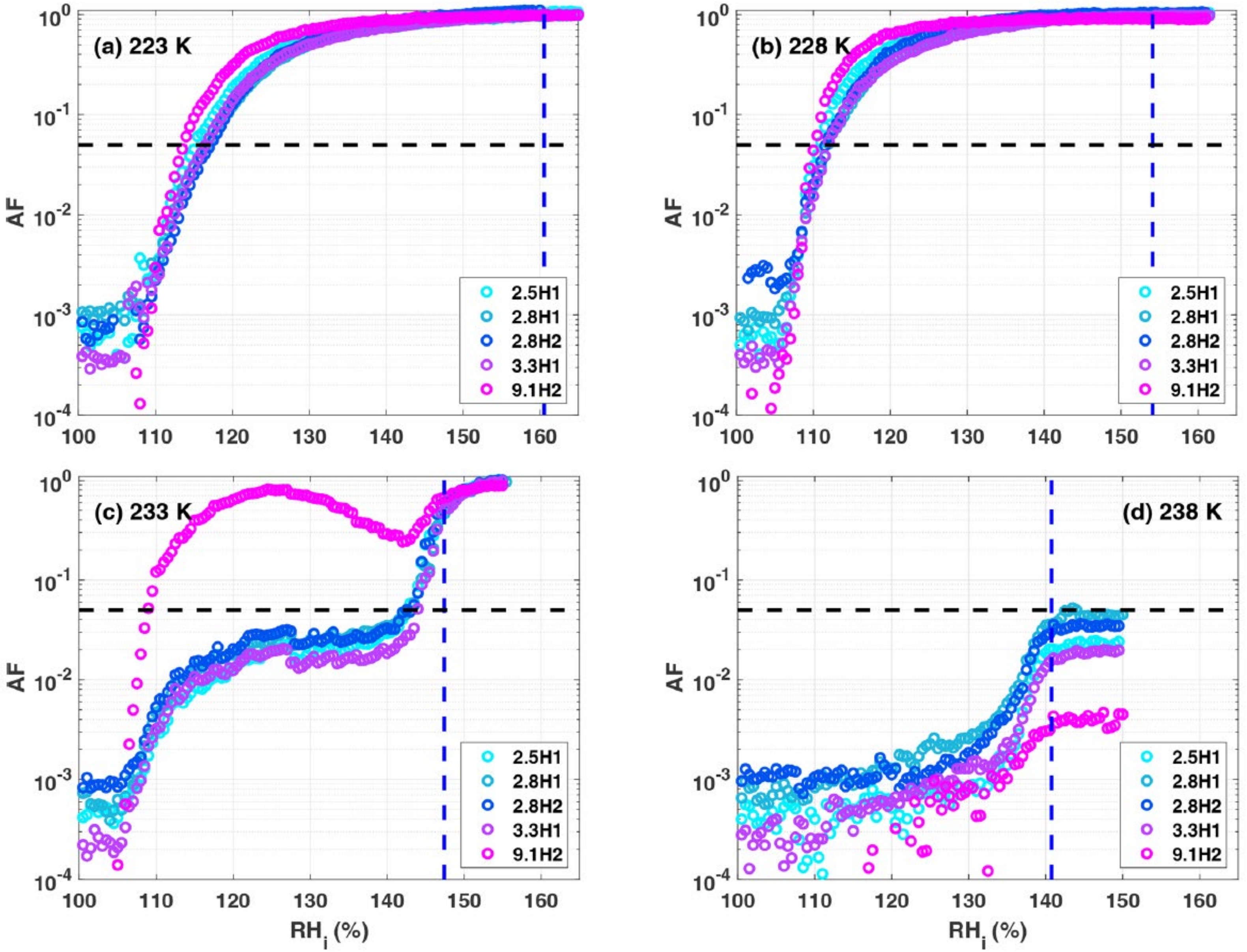

David et al., 2020

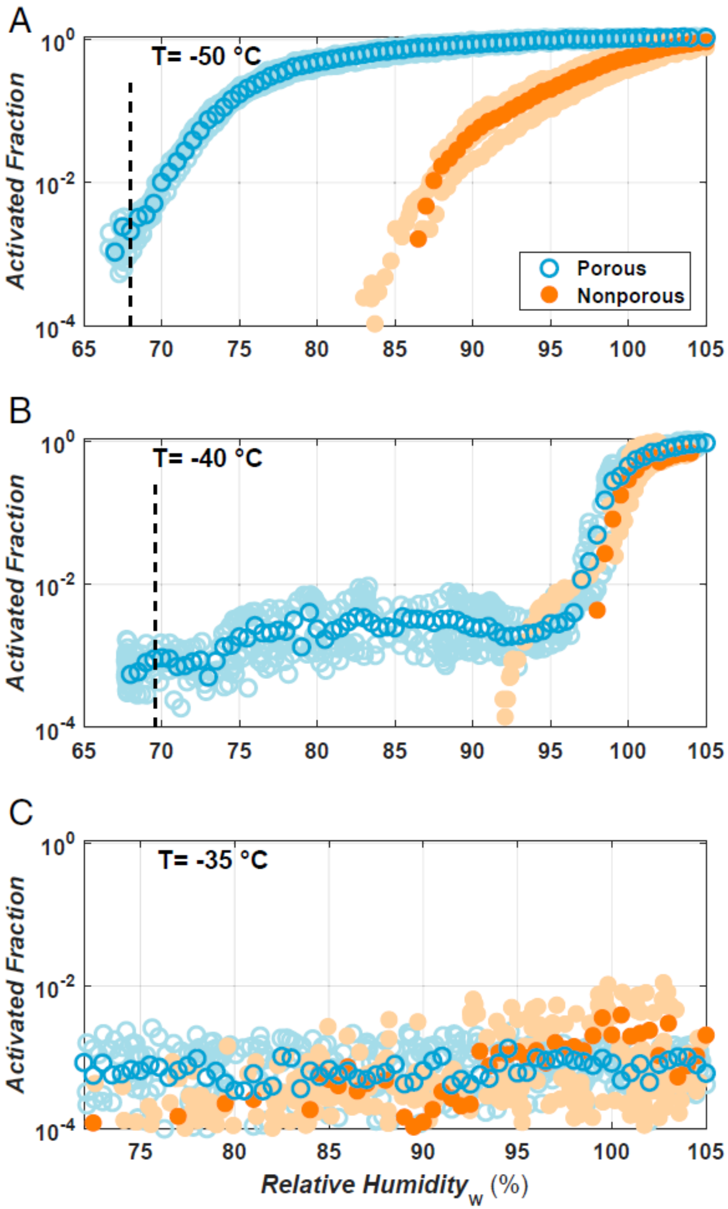

Calcined particles
Pore diameter: 3.8 nm

PCF:
Homogeneous ice nucleation within pores

Homogeneous condensation freezing

No ice nucleation above the homogeneous ice nucleation threshold

David et al., 2019

What evidence is required for PCF

- Increase in activated fraction when temperature falls below the homogeneous ice nucleation threshold ✓
- Presence of pores in ice-nucleating particles ✓
- Pore condensation occurring well below water saturation
- Ability of ice to nucleate within very small water volumes
- Ability of ice to grow out of the pores from the vapor phase

Pore condensation and freezing (PCF): capillary condensation

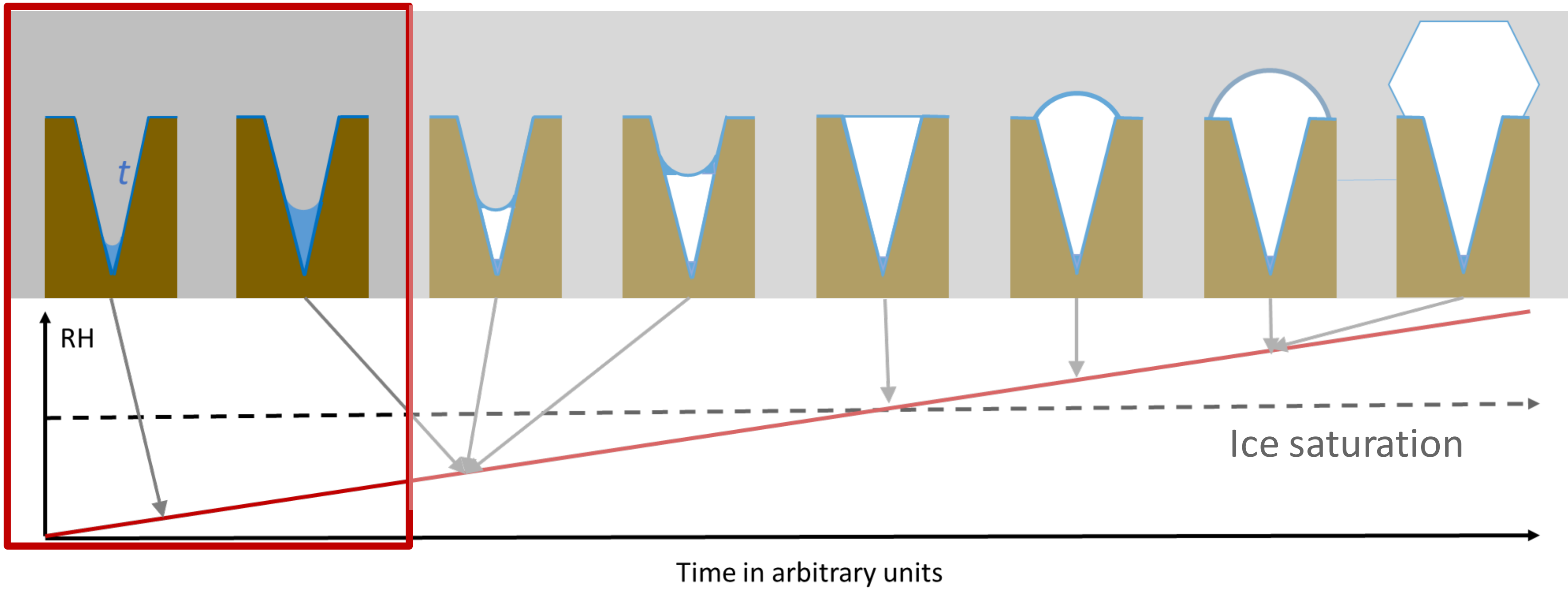

Water condensation in pores

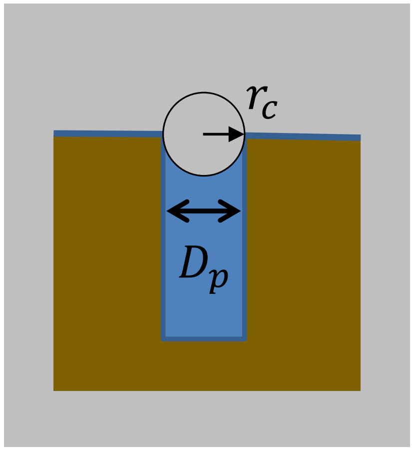

Radius of curvature

$$r_c = \frac{-D_p}{2}$$

Kelvin equation

$$\frac{p}{p_w} = exp\left(\frac{-4\gamma_{vw} v_w}{D_p kT}\right)$$

p : water vapor pressure above concave surface
p_w: water vapor pressure over flat water surface
γ_{vw}: surface tension of water
v_w: molecular volume of water
D_p: pore diameter
k: Boltzmann constant
T: absolute temperature.

Water sorption isotherms of mesoporous silica materials

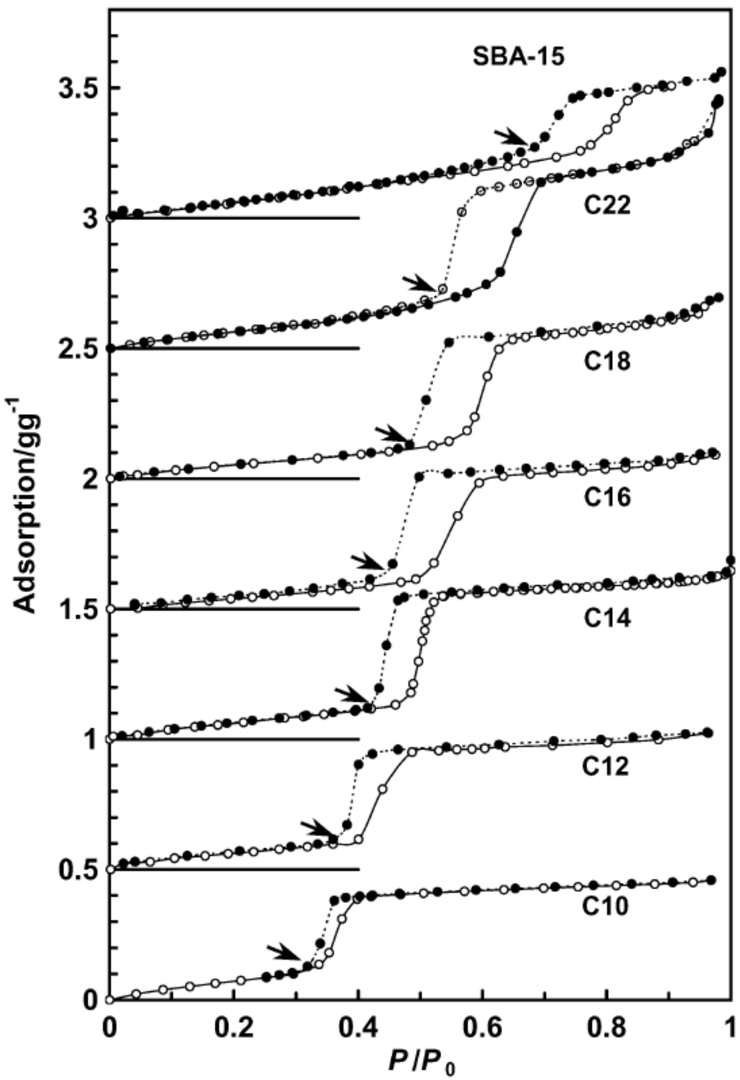

Pore diameter

8.69 nm

4.19 nm

3.60 nm

3.11 nm

2.83 nm

2.38 nm

2.10 nm

Kittaka et al., 2006

Onset of capillary condensation from water sorption isotherms

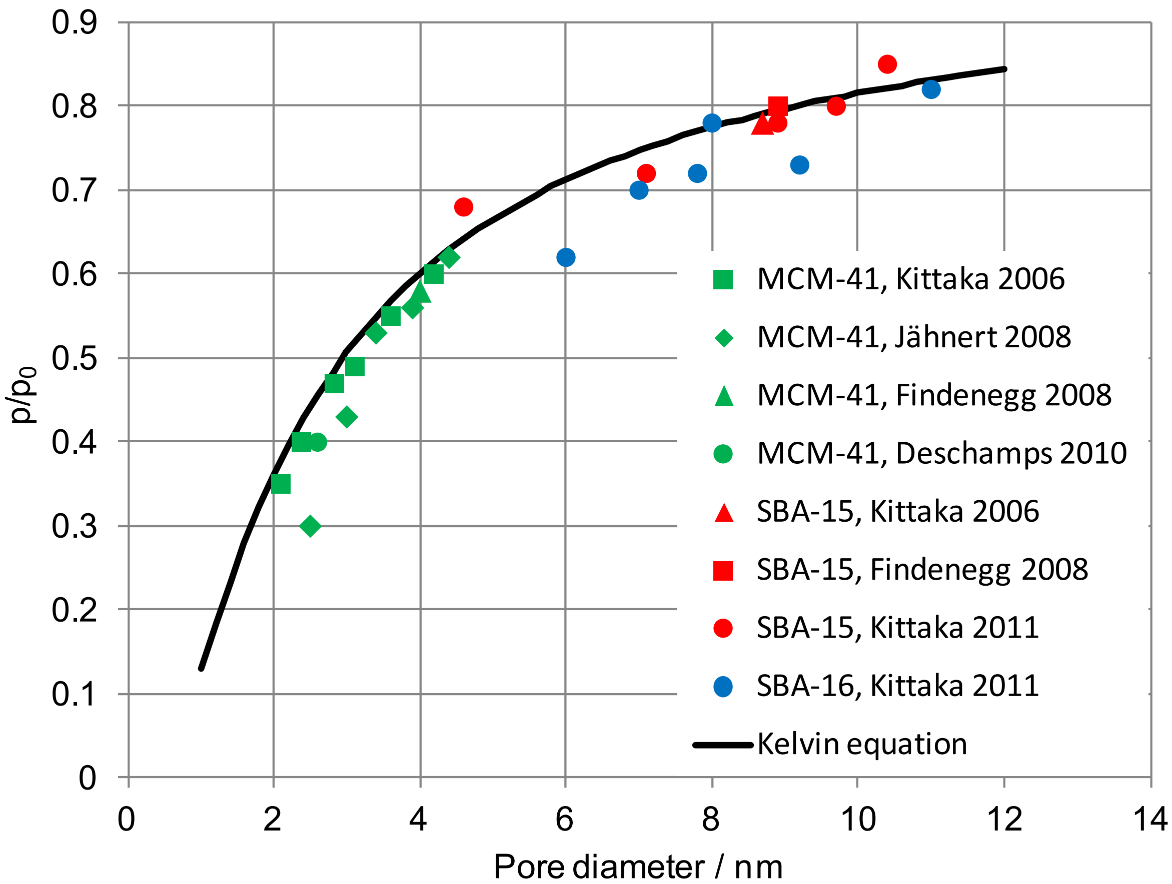

Data from:

- Kittaka et al., 2006 (measured gravimetrically at 25°C)
- Jähnert et al., 2008 (DVS (dynamic vapor sorption) at 20°C)
- Findenegg et al., 2008 (measurements at 20°C)
- Deschamps et al., 2010 (DVS
- Kittaka et al., 2011 (measured gravimetrically)
- The black solid line indicates the onset of capillary condensation predicted by the Kelvin equation (for T = 298 K).

Kelvin equation:

$$\frac{p}{p_w} = exp\left(\frac{-4\gamma_{vw}v_w}{D_p kT}\right)$$

Marcolli, 2014

Water condensation in pores

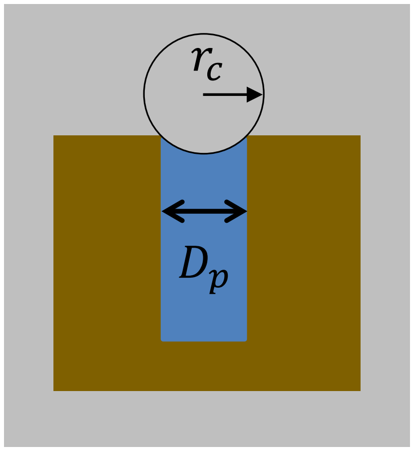

Radius of curvature:

$$r_c = \frac{-D_p}{2\cos\theta_{ws}}$$

Kelvin equation

$$\frac{p}{p_w} = exp\left(\frac{-4\gamma_{vw}v_w\cos\theta_{ws}}{D_p kT}\right)$$

p : water vapor pressure above concave surface
p_w: water vapor pressure over flat water surface
γ_{vw}: surface tension of water
v_w: molecular volume of water
D_p: pore diameter
k: Boltzmann constant
T: absolute temperature
θ_{ws}: contact angle between water and pore surface

Dependence of freezing onsets on contact angle

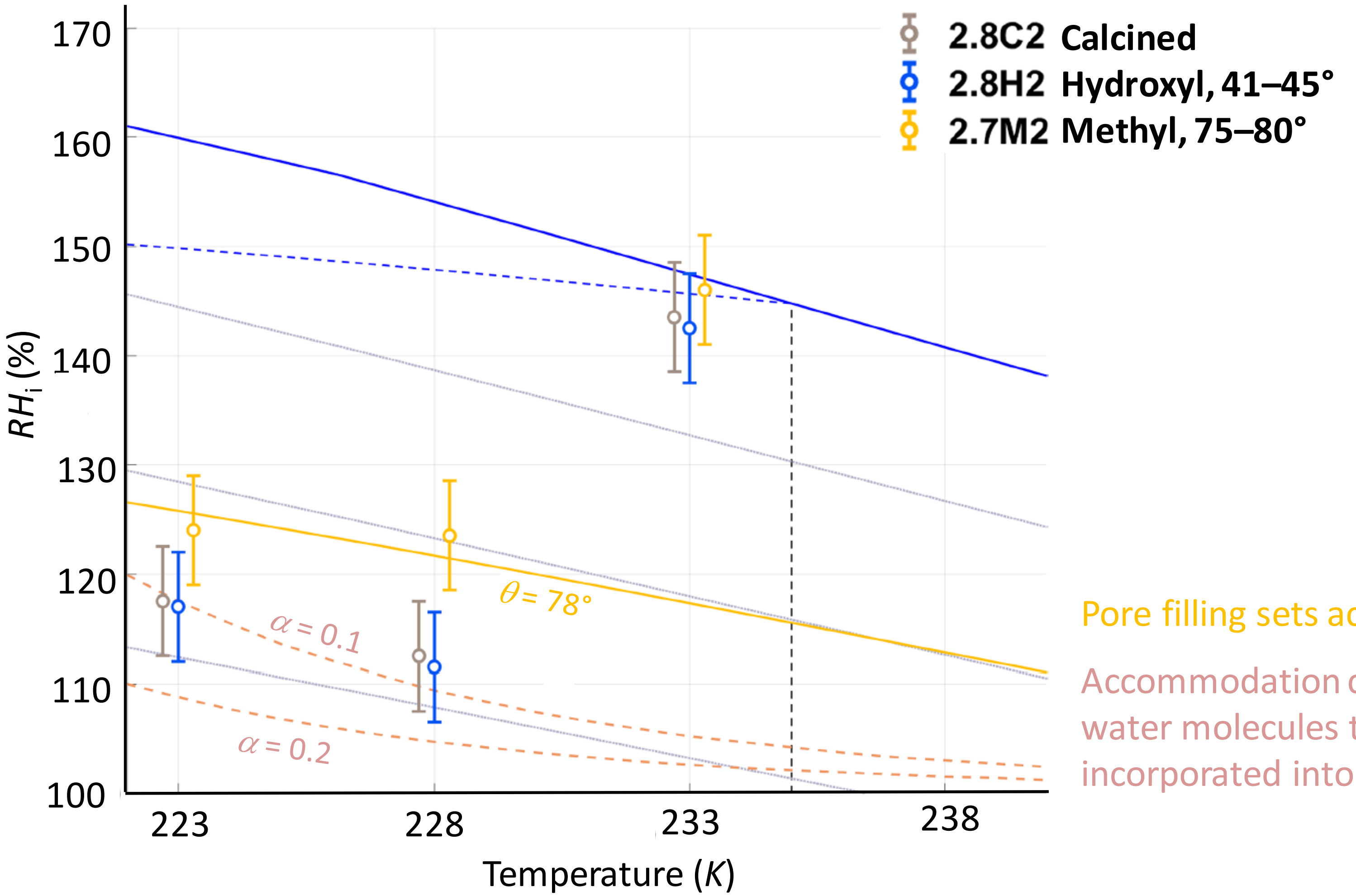

Pore filling sets activation barrier

Accommodation coefficient for water molecules to be incorporated into the ice lattice

David et al., 2020

Water condensation in conical and wedge-shaped pores

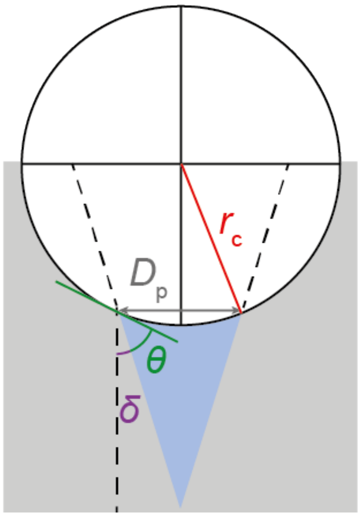

Radius of curvature:

$$r_c = \frac{-D_p}{2\cos(\theta_{ws} + \delta)}$$

Kelvin equation

$$\frac{p}{p_w} = exp\left(\frac{-4\gamma_{vw} v_w \cos(\theta_{ws} + \delta)}{D_p kT}\right)$$

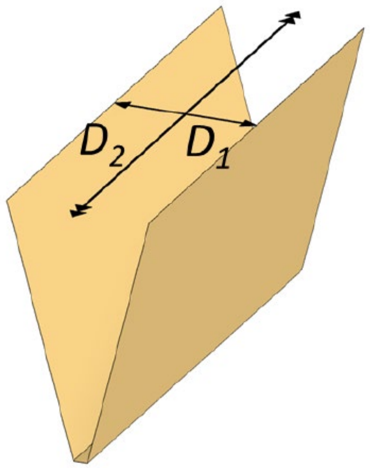

Radii of curvature:

$$r_{c1} = \frac{-D_1}{2\cos(\theta_{ws} + \delta)} \qquad r_{c2} = \infty$$

Kelvin equation:

$$\frac{p}{p_w} = exp\left(\frac{\gamma_{vw} v_w \left(\frac{1}{r_{c1}} + \frac{1}{r_{c2}}\right)}{D_1 kT}\right)$$

$$\frac{p}{p_w} = exp\left(\frac{-2\gamma_{vw}\, v_w \cos(\theta_{ws} + \delta)}{D_1 kT}\right)$$

Marcolli, 2020

Effect of contact angle and opening angle on pore filling

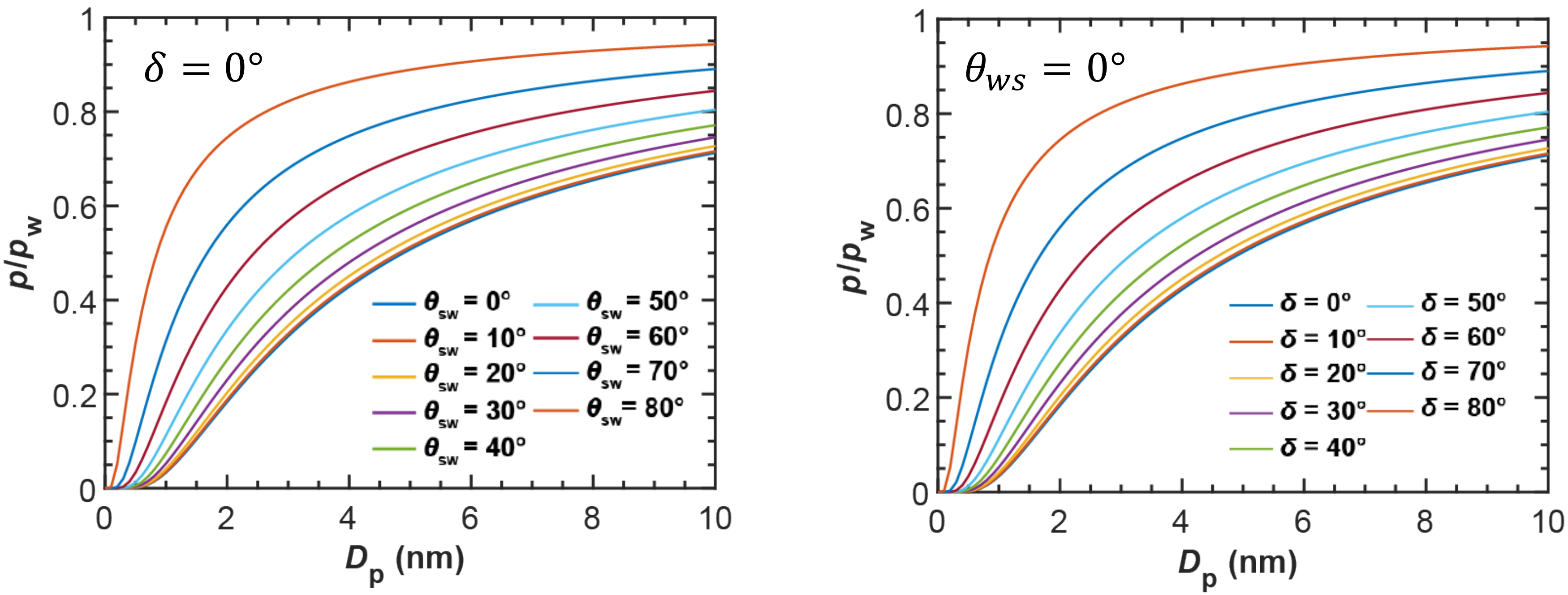

Kelvin equation
$$\frac{p}{p_w} = exp\left(\frac{-4\gamma_{vw}\cos(\theta_{ws}+\delta)}{D_p kT}\right)$$

→ The contact angle θ_{ws} and the pore opening angle δ have the same effect on $\frac{p}{p_w}$

Pore condensation and freezing (PCF): ice nucleation

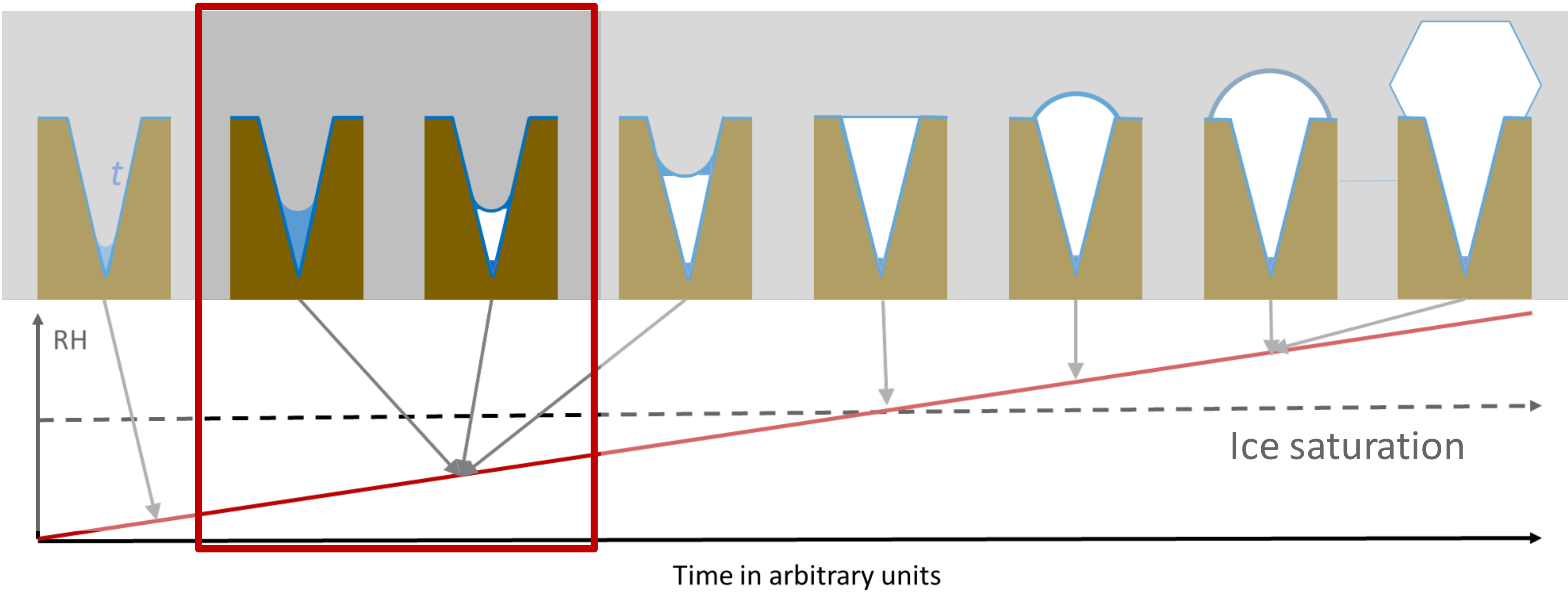

Pore condensation and freezing (PCF): ice nucleation

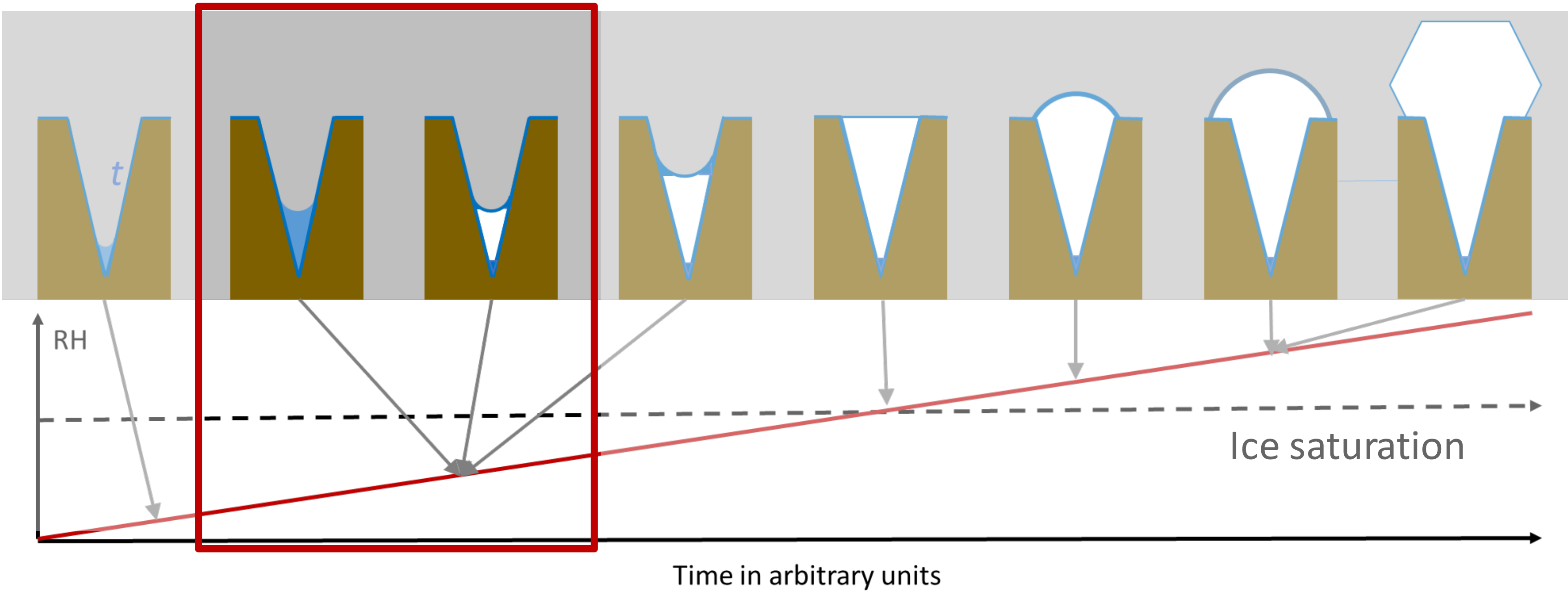

Number of pores	Pore diameter	liquid layer thickness	Pore length	Volume	Nucleation rate required
1	3 nm	0.38 nm	3 nm	16 nm^3	$6 \cdot 10^{19}\ cm^{-3}s^{-1}$
1	3 nm	0.38 nm	500 nm	2696 nm^3	$4 \cdot 10^{17}\ cm^{-3}s^{-1}$
100	3 nm	0.38 nm	500 nm	269564 nm^3	$4 \cdot 10^{15}\ cm^{-3}s^{-1}$

Freezing of micrometer-sized droplets

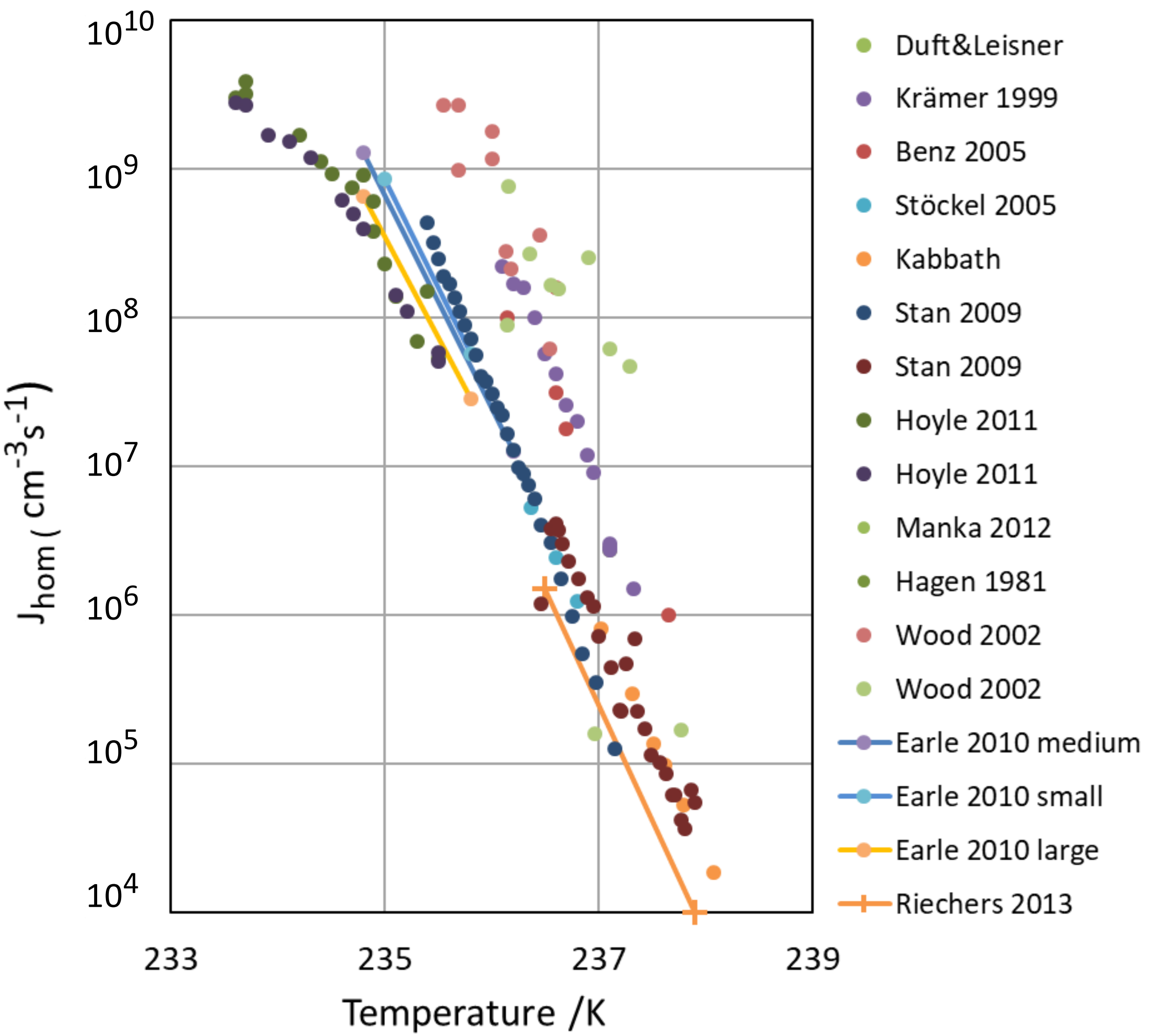

Freezing of nanodroplets from supersonic nozzle experiments

Bartell & Chusak, 1994
nanodroplets:
3.4 nm radius

Bhabhe et al., 2013
nanodroplets:
3 – 9 nm radius, 30–50 MPa

Manka et al., 2012
nanodroplets:
3.2 – 5.8 nm radius

Amaya and Wyslouzil, 2018
nanodroplets:
6.6 – 10 nm radius), ~17 MPa

Laksmono et al., 2015
Ultrafast cooling:
$10^3 – 10^4$ K/s

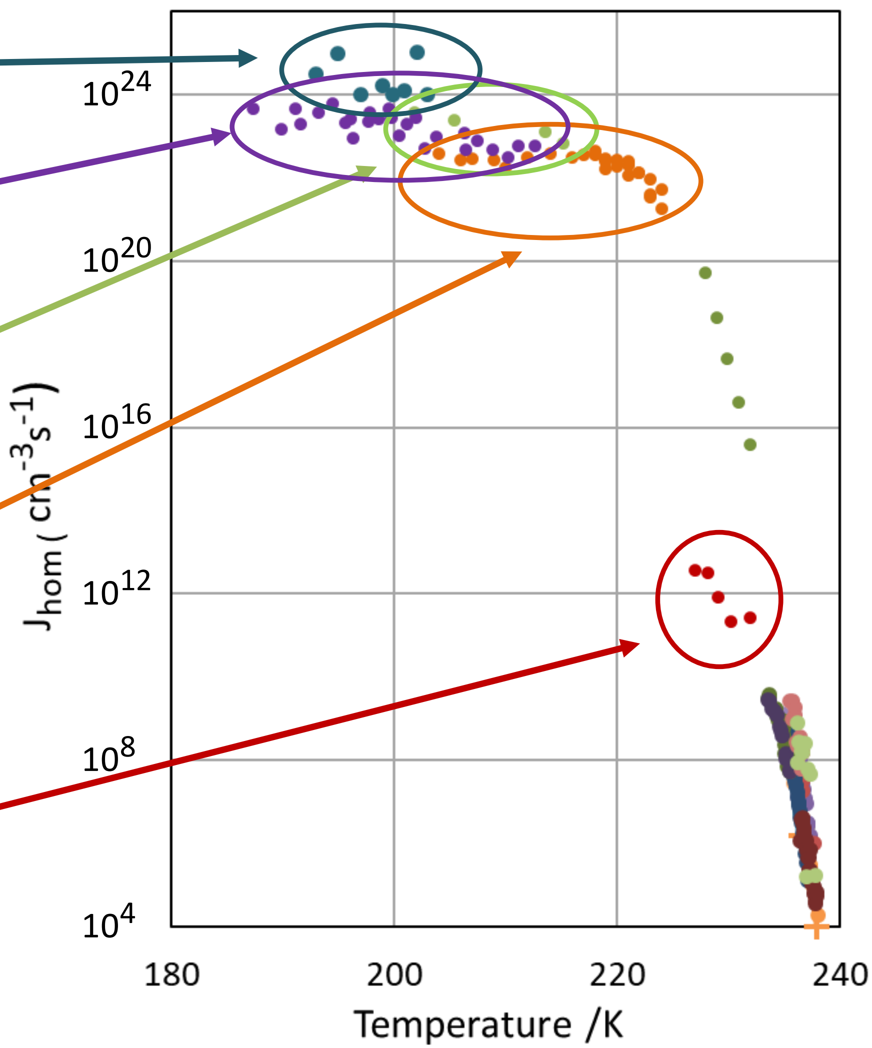

Classical Nucleation Theory (CNT)

$$\Delta G = 4\pi\gamma_{iw}(T)r^2 - \frac{4\pi r^3}{3v_i} kT ln\left(\frac{p_w}{p_i}\right)$$

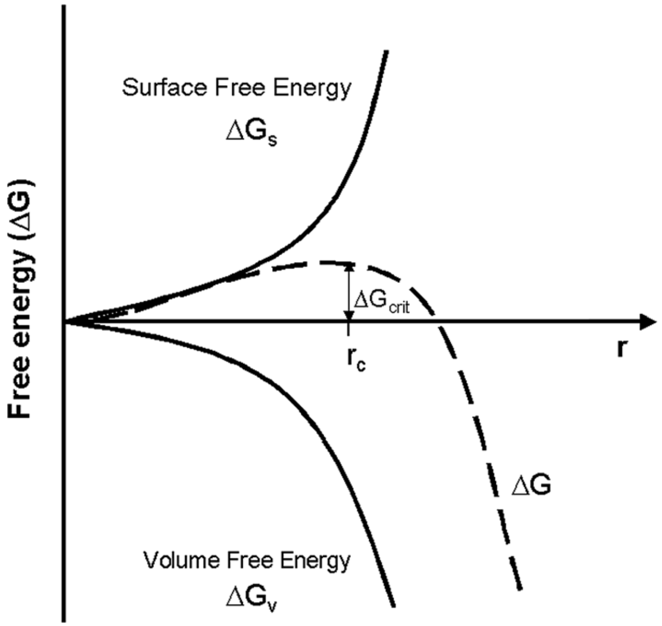

$\gamma_{iw}(T)$: interfacial tension ice/water

$\frac{p_w}{p_i}$: supersaturation

Critical nucleus shape in an MD simulation

Cubic ice cluster (~4000 molecules) inserted in supercooled water (TIP4P/Ice) .

The inserted cluster exposes the (100), (010), and (001) planes to the fluid.

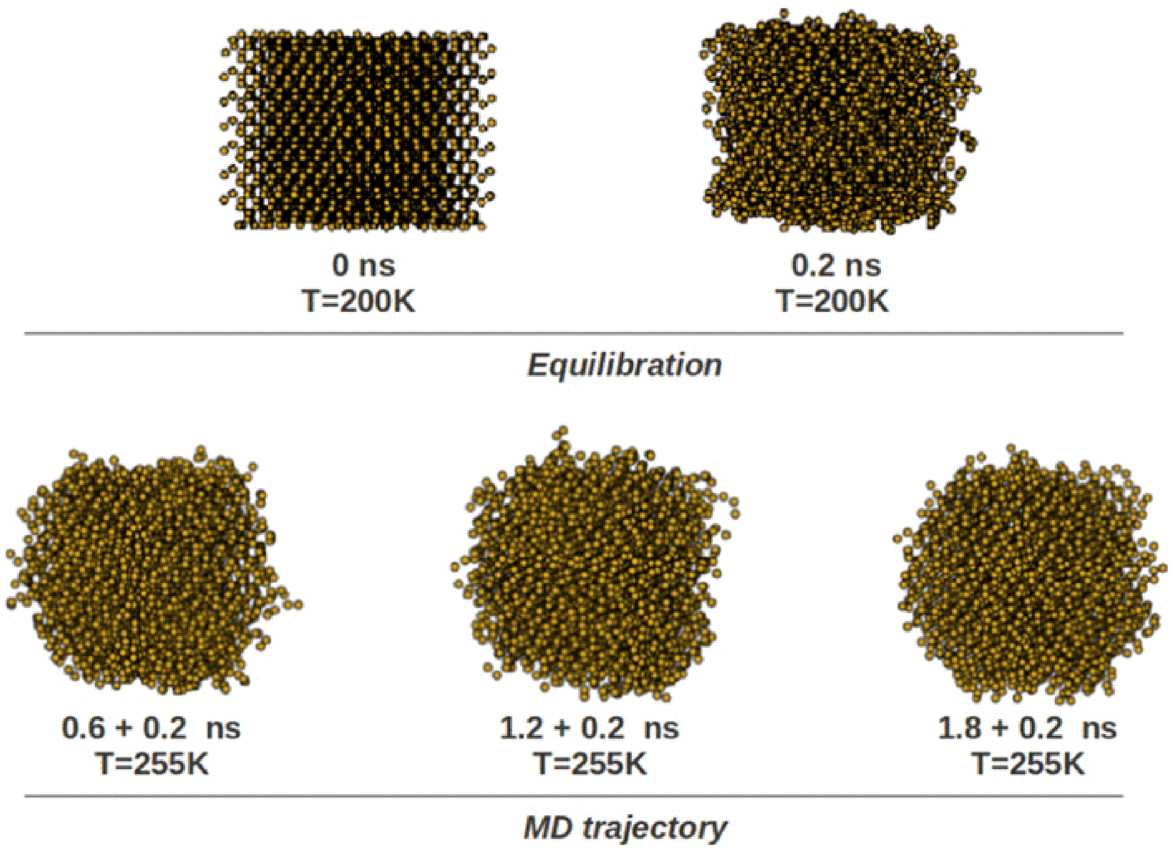

Equilibration of the interface for 0.2 ns at 200 K

Let cluster evolve at 255 K (temperature at which a cluster of this size should be critical)

→ cluster turns spherical to minimize interfacial free energy.

Zaragoza et al., 2015

Classical Nucleation Theory (CNT)

$$\Delta G = 4\pi\gamma_{iw}(T)r^2 - \frac{4\pi r^3}{3v_i}kT\ln\left(\frac{p_w}{p_i}\right)$$

Determine ΔG_{crit} i.e. maximum of ΔG:

$$\frac{\Delta G}{dr} = 8\pi\gamma_{iw}(T)r - \frac{4\pi r^2}{v_i}kT\ln\left(\frac{p_w}{p_i}\right) = 0$$

→ Critical radius $r_{crit} = \dfrac{2\gamma_{iw}(T)v_i}{kT\ln\frac{p_w}{p_i}}$

→ Energy barrier $\Delta G_{crit} = \dfrac{16\pi\gamma_{iw}(T)^3 v_i^2}{3k^2T^2\left(\ln\left(\frac{p_w}{p_i}\right)\right)^2}$

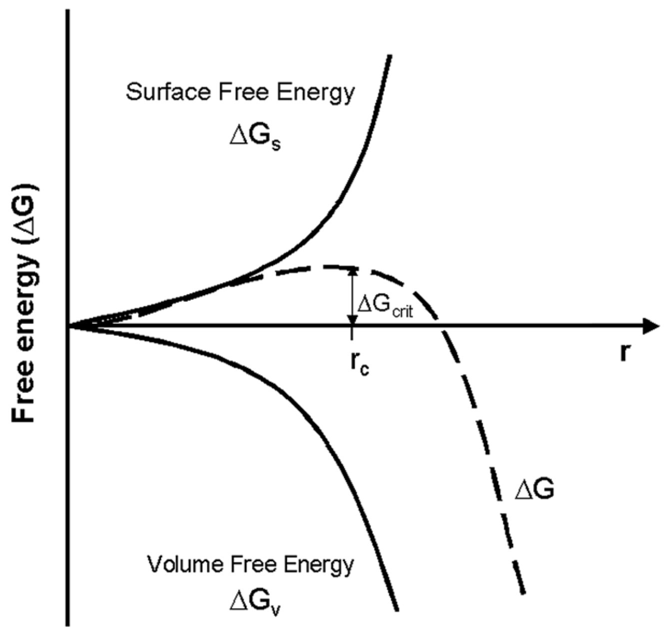

$\gamma_{iw}(T)$: interfacial tension ice/water

$\frac{p_w}{p_i}$: supersaturation

Classical Nucleation Theory (CNT)

$$\Delta G = 4\pi\gamma_{iw}(T)r^2 - \frac{4\pi r^3}{3v_i}kTln\left(\frac{p_w}{p_i}\right)$$

Determine ΔG_{crit} i.e. maximum of ΔG:

$$\frac{\Delta G}{dr} = 8\pi\gamma_{iw}(T)r - \frac{4\pi r^2}{v_i}kTln\left(\frac{p_w}{p_i}\right) = 0$$

→ Critical radius $$r_{crit} = \frac{2\gamma_{iw}(T)v_i}{kTln\frac{p_w}{p_i}}$$

→ Energy barrier $$\Delta G_{crit} = \frac{16\pi\gamma_{iw}(T)^3 v_i^2}{3k^2T^2\left(ln\left(\frac{p_w}{p_i}\right)\right)^2}$$

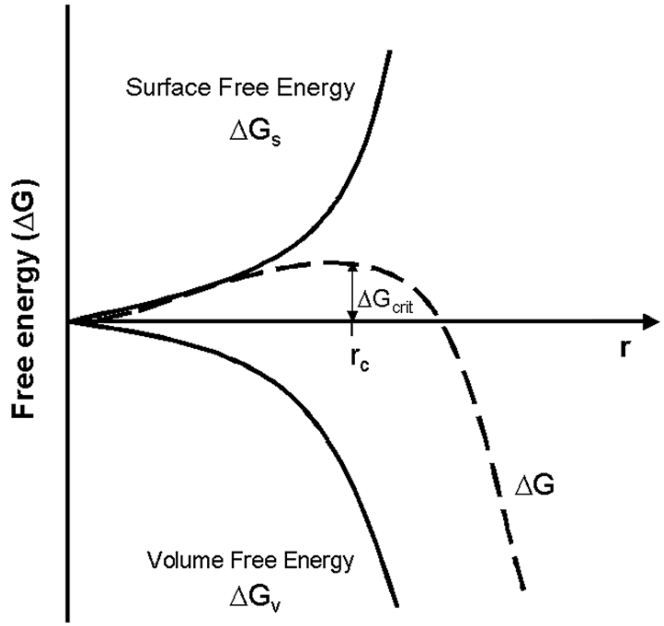

$\gamma_{iw}(T)$: interfacial tension ice/water

$\frac{p_w}{p_i}$: saturation ratio

ΔF_{diff}: diffusional energy barrier

Homogeneous ice nucleation rate: $$J_{hom} = \frac{kT}{h}exp\left(\frac{\Delta F_{diff}}{kT}\right)n_v\exp\left(-\frac{\Delta G_{hom}}{kT}\right)$$

Interfacial tension ice/water

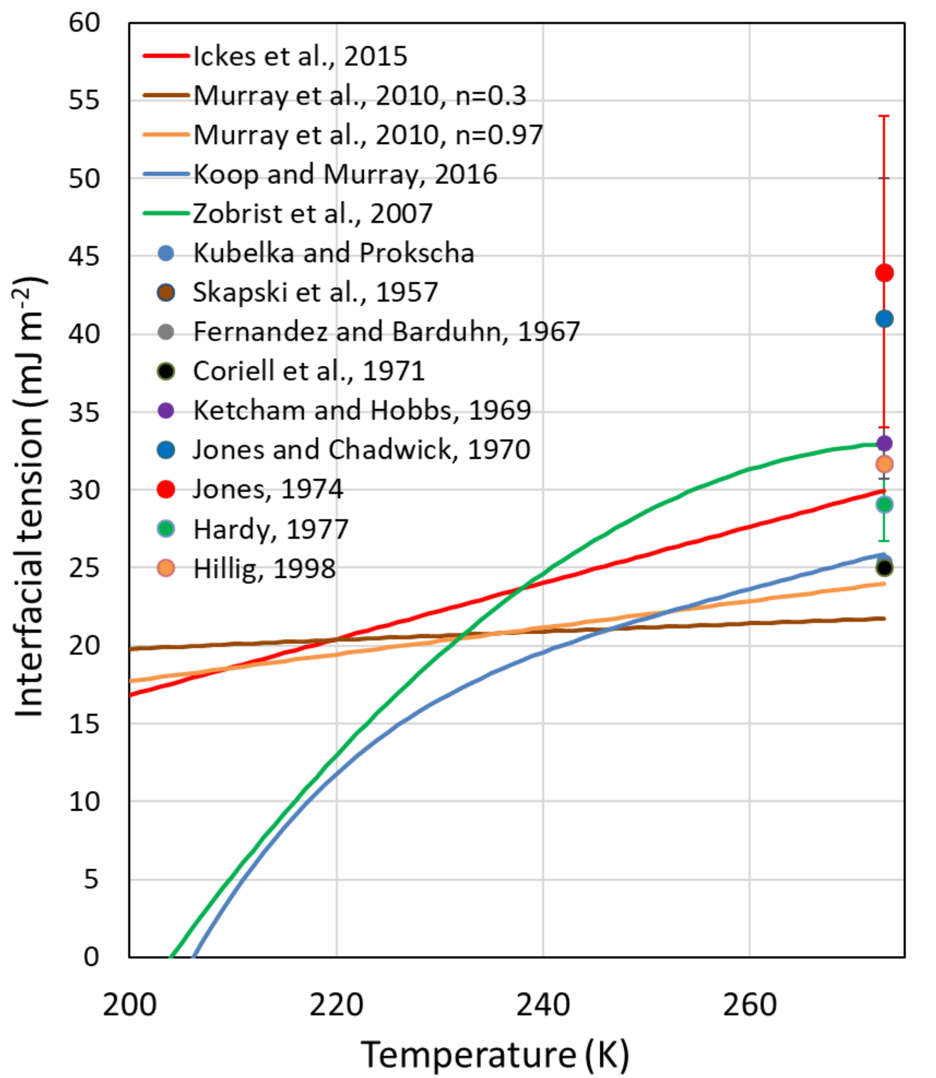

Zobrist et al., 2007: hexagonal ice, fit to ice nucleation rates

Ickes et al., 2015: hexagonal ice, linear extrapolation

Koop and Murray, 2016:

Stacking disordered ice; temperature dependence of interfacial tension is scaled to the temperature dependence of the enthalpy of melting, based on Turnbull correlation:

$\gamma_{iw}(T_{hom}) \propto \Delta H_m (T_m)$

Murray et al., 2010:

Stacking disordered ice

$$\gamma_{iw}(T) = \gamma_{iw}(T_0)\left(\frac{T}{T_0}\right)^n$$

T_0 : homogeneous ice nucleation temperature

Parameterizations of ice nucleation rates

Zobrist et al., 2007

Murray et al., 2010, n = 0.97

Murray et al., 2010, n = 0.3

Ickes et al., 2015

Koop and Murray, 2016

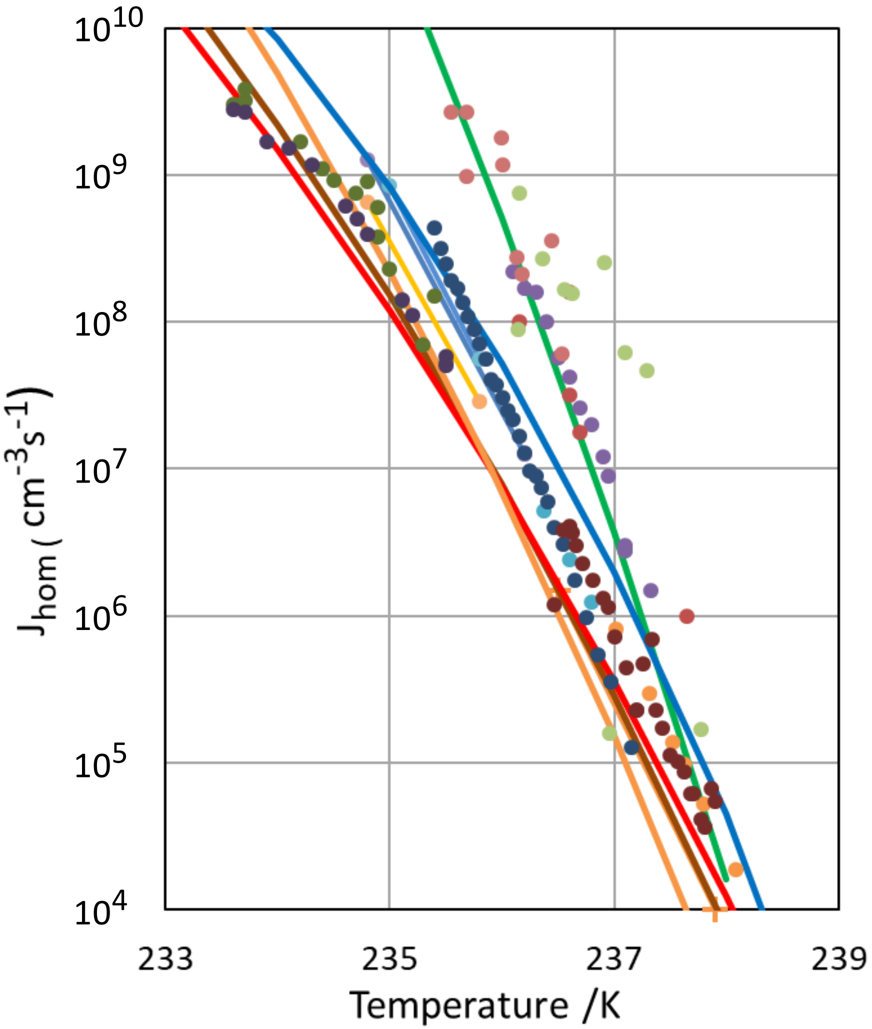

Parameterizations of ice nucleation rates

Zobrist et al., 2007

Murray et al., 2010, *n* = 0.97

Murray et al., 2010, *n* = 0.3

Ickes et al., 2015

Koop and Murray, 2016

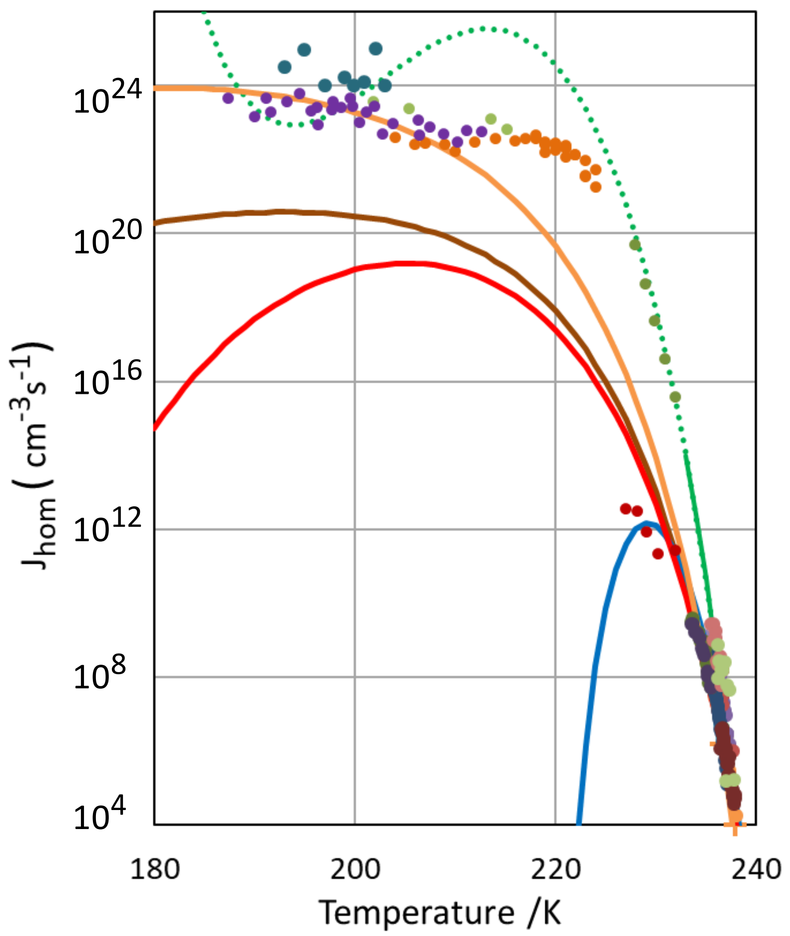

Parameterizations of ice nucleation rates

Zobrist et al., 2007
Murray et al., 2010, n = 0.97
Murray et al., 2010, n = 0.3
Ickes et al., 2015
Koop and Murray, 2016

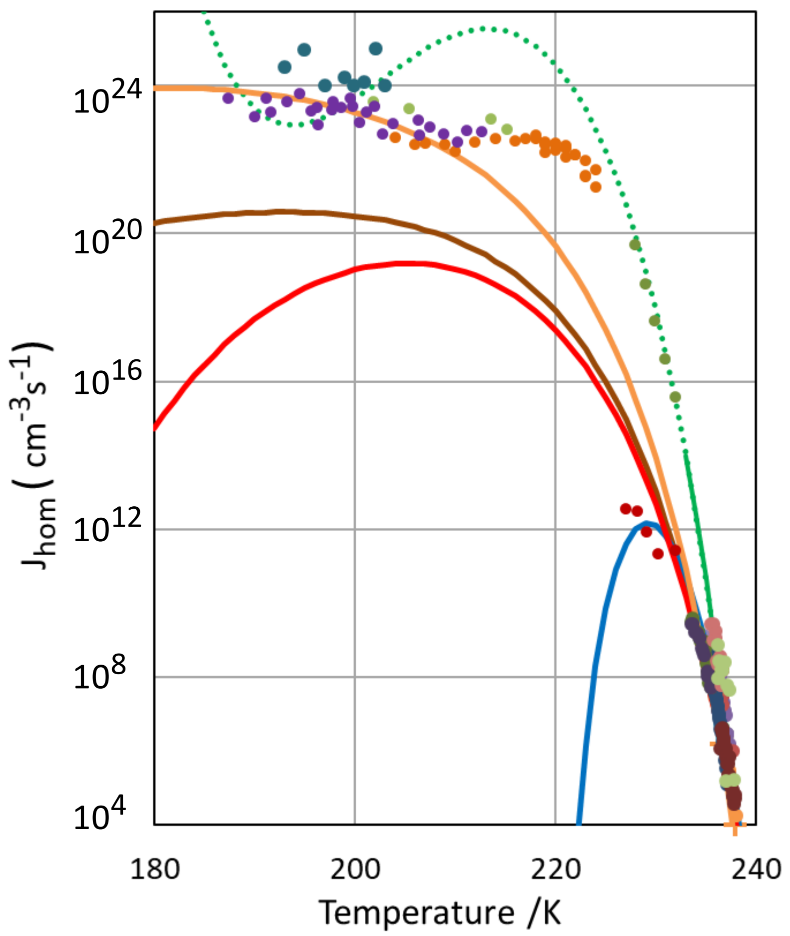

Critical nucleus size

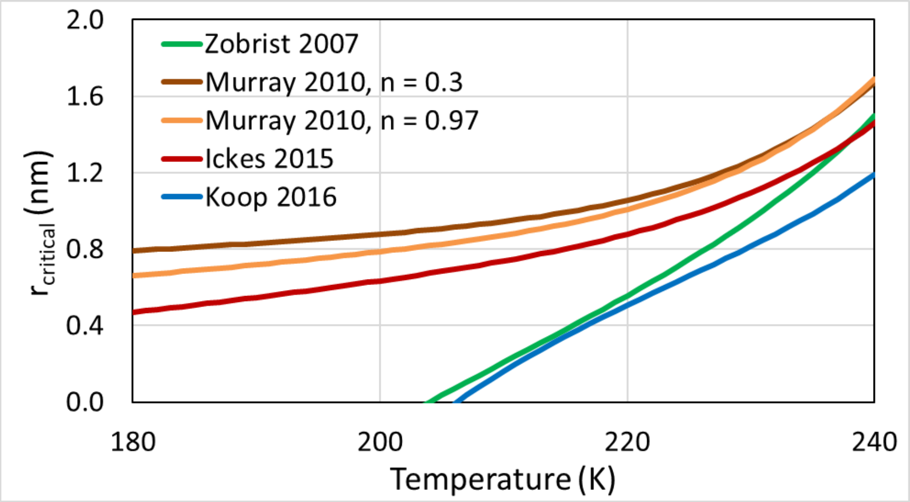

Homogeneous freezing temperature in solution and under pressure

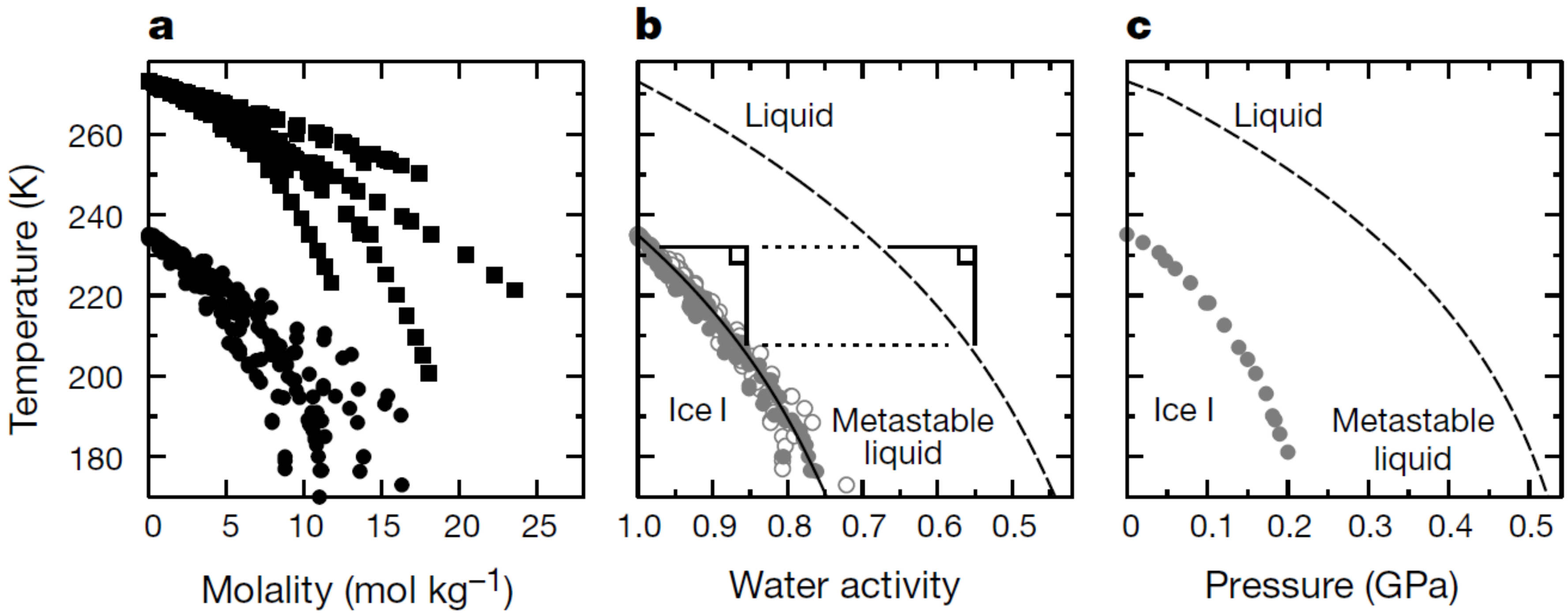

Koop et al., Nature, 2000

Homogeneous ice nucleation as a function of pressure

Melting curve $\mu_i(T,P) = \mu_w(T,P)$

$$(P-P_0)v_i(T,P_0) + kTln\big(p_i(T,P_0)\big) = (P-P_0)\frac{v_w(T,P)+v_w(T,P_0)}{2} + kTln\big(p_w(T,P_0)\big)$$

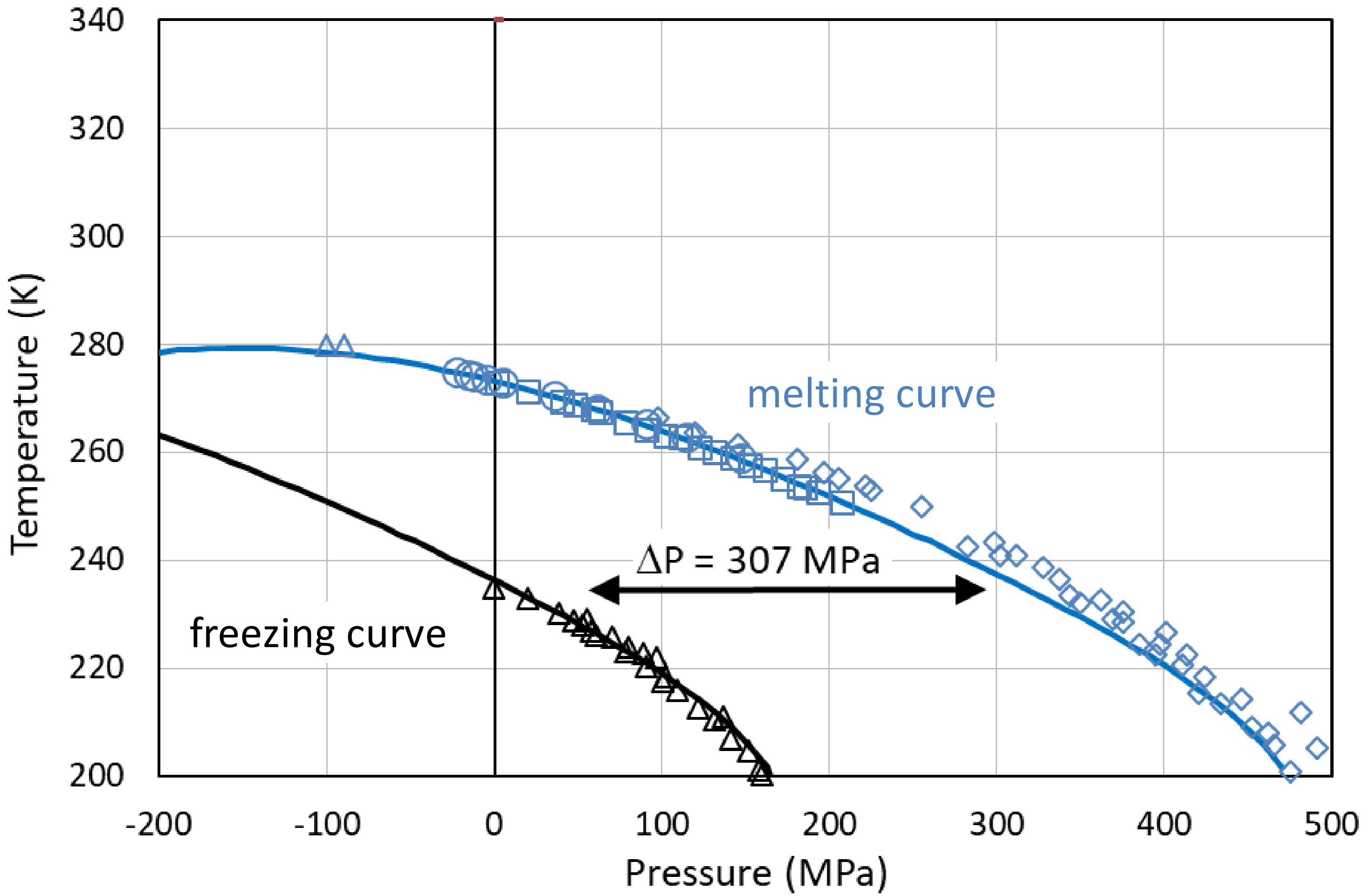

Marcolli, 2017, 2020

Homogeneous ice nucleation as a function of pressure

Melting curve $\mu_i(T,P) = \mu_w(T,P)$

$$(P-P_0)v_i(T,P_0) + kTln\big(p_i(T,P_0)\big) = (P-P_0)\frac{v_w(T,P)+v_w(T,P_0)}{2} + kTln\big(p_w(T,P_0)\big)$$

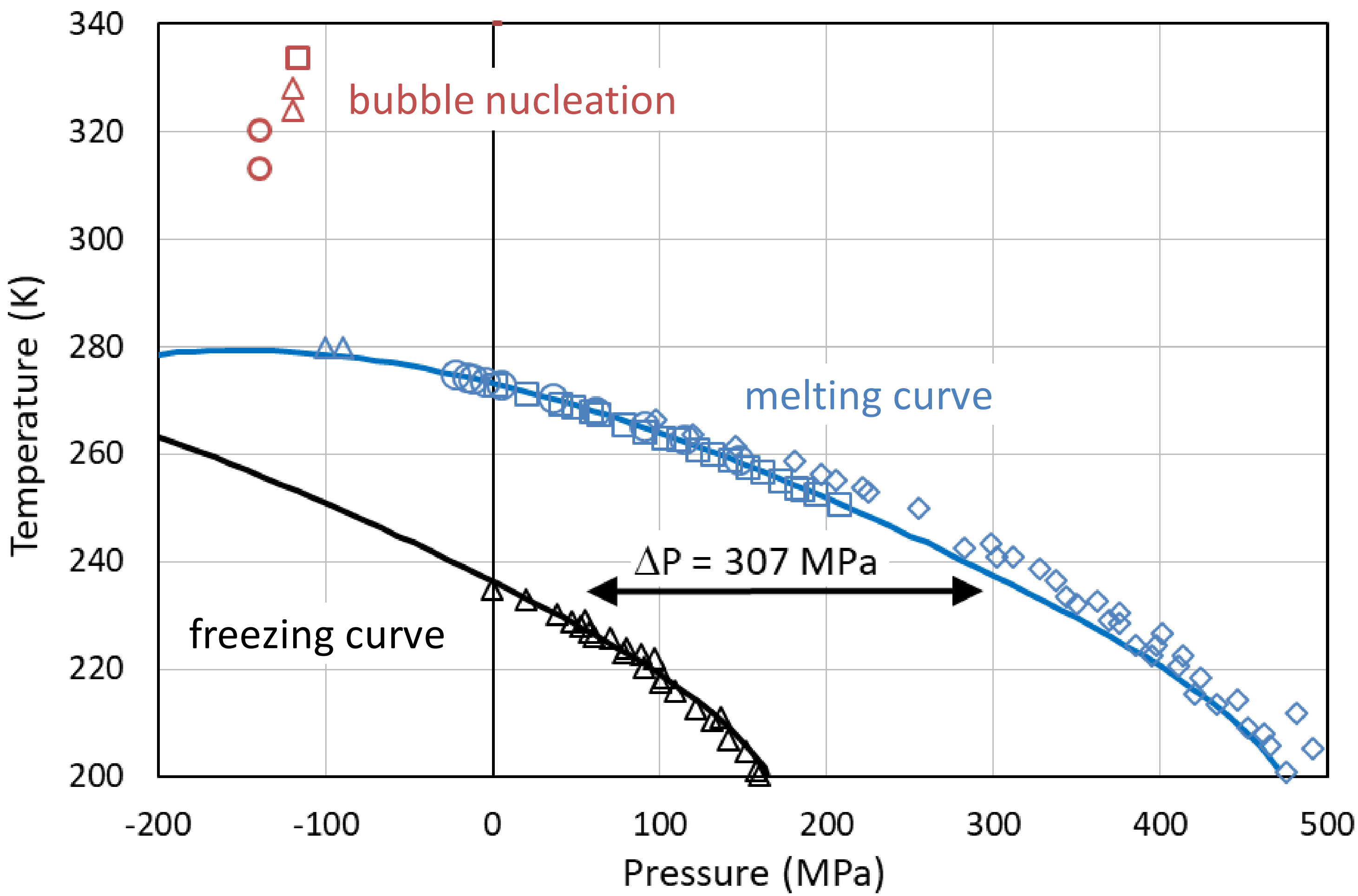

Marcolli, 2017, 2020

Homogeneous bubble nucleation described by CNT

The evolution of the free energy during bubble formation is given by

$$\Delta G_{bw} = 4\pi r_b^2 \gamma_{bw} - \frac{4\pi r_b^3}{3\nu_l}(\mu_l - \mu_b).$$

the difference in chemical potential can be expressed as the ratio of vapor pressures and making use of the Laplace-Kelvin equation:

$$\mu_l - \mu_b = kT ln \frac{p_l}{p_b} = \nu_l (p_l - P_{ex})$$

Yielding the critical radius and the energy barrier:

$$r_{b,cr} = \frac{2\gamma_{bw}}{(p_l - P_{ex})} \qquad \Delta G_{bw,cr} = \frac{16\pi\gamma_{bw}^3}{3(p_l - P_{ex})^2}$$

and the rate per volume and time:

$$j_{bw,hom} = n_v \left(\frac{2\sigma_{bw}}{\pi m B}\right)^{1/2} exp\left(\frac{-\Delta G_{bw,cr}}{kT}\right)$$

Symbols:

r_b: radius of the evolving bubble

γ_{bw}: surface tension of water

μ_b: chemical potential of water molecules in the bubble

μ_l: chemical potential of the molecules in liquid water at normal pressure

ν_l: molecular volume of liquid water

p_l,: vapor pressures of liquid water

p_b: vapor pressure in the bubble

P_{ex},: pressure applied to the liquid

Homogeneous ice nucleation as a function of pressure

Melting curve $\mu_i(T,P) = \mu_w(T,P)$

$$(P-P_0)v_i(T,P_0) + kTln\big(p_i(T,P_0)\big) = (P-P_0)\frac{v_w(T,P)+v_w(T,P_0)}{2} + kTln\big(p_w(T,P_0)\big)$$

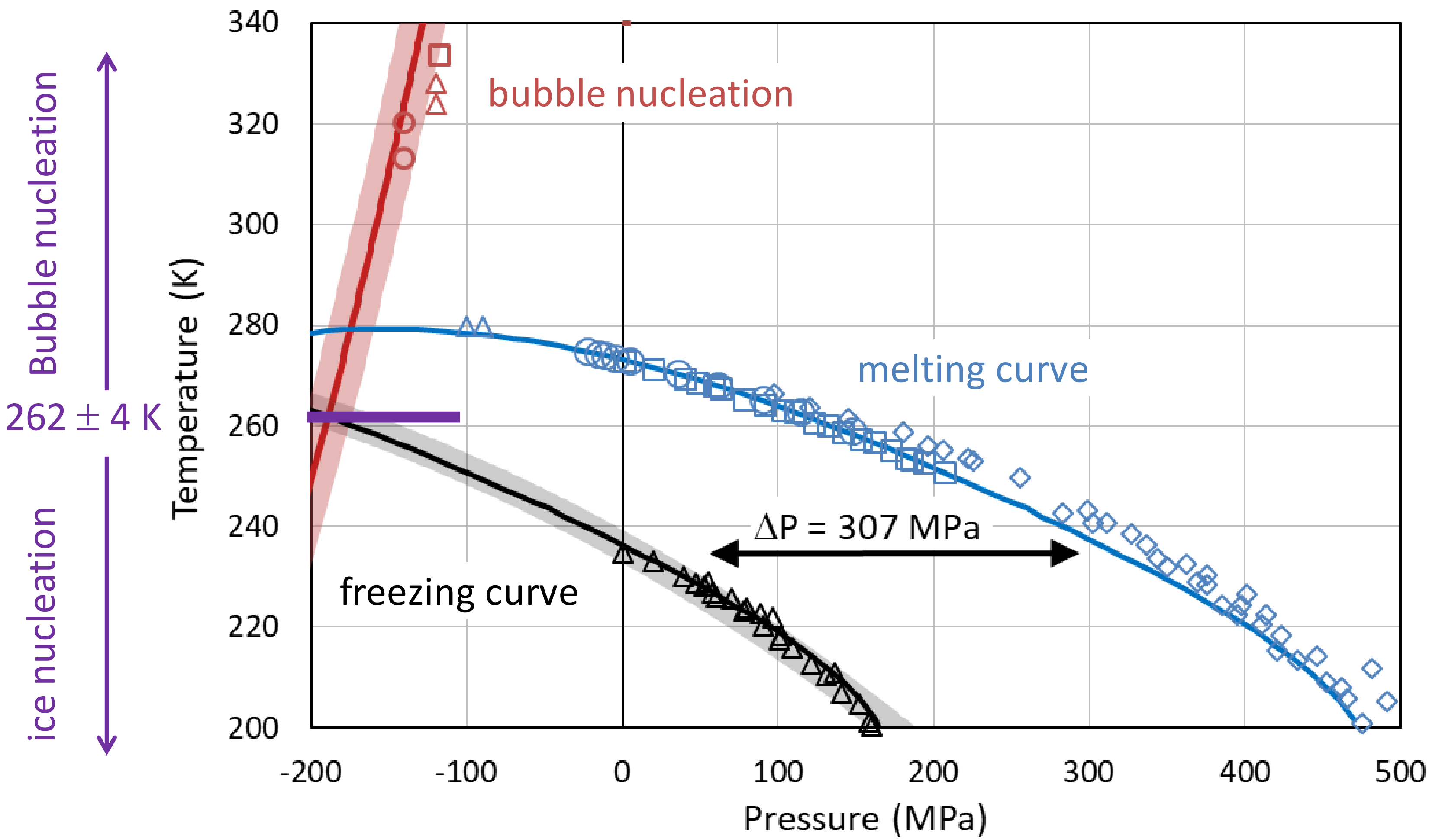

Marcolli, 2017, 2020

Parameterization of pressure dependent ice nucleation rates

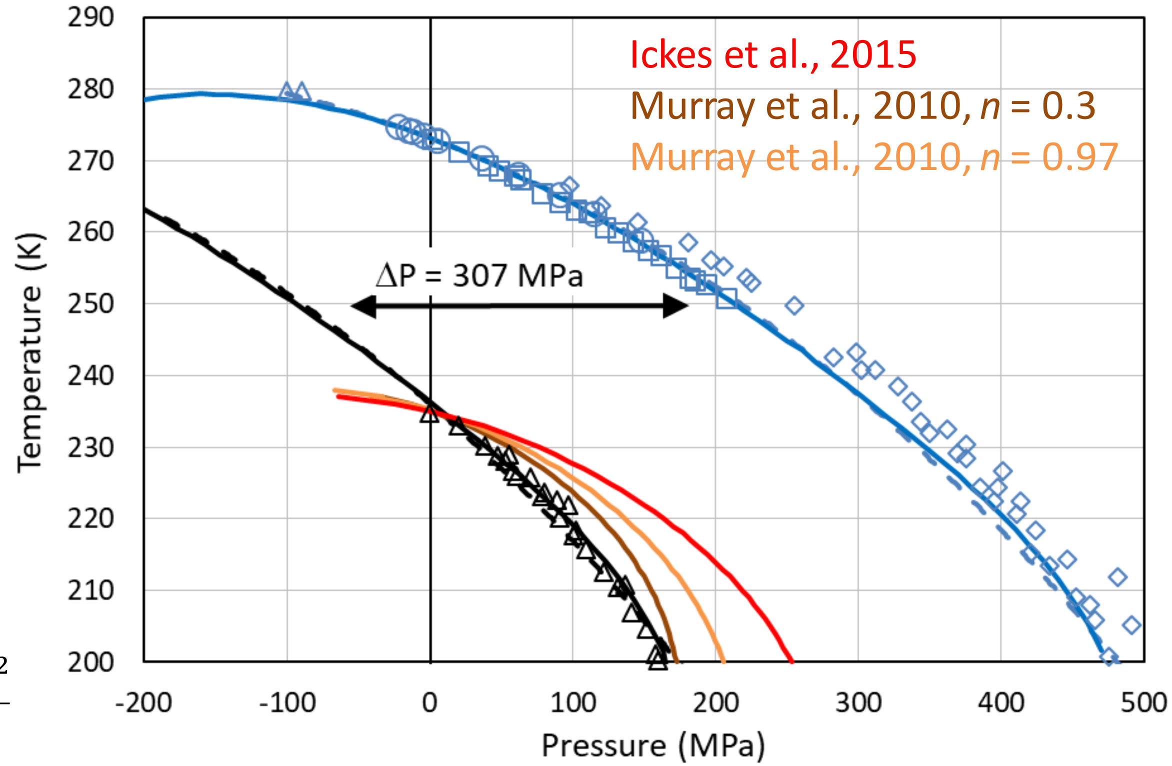

$$\Delta G_c(T,P) = \frac{16\pi\gamma_{iw}(T,P)^3 v_i(T,P_0)^2}{3(\mu_w - \mu_i)^2}$$

$$\Delta G_c(T,P) = \frac{16\pi\gamma_{iw}(T,P)^3 v_i(T,P_0)^2}{3\left(kTln\left(\frac{p_w(T,P_0)}{p_{ih}(T,P_0)}\right) - (P-P_0)v_i(T,P_0) + (P-P_0)\frac{v_w(T,P)+v_w(T,P_0)}{2}\right)^2}$$

$$J_{hom} = C_{prefac}\exp\left(\frac{\Delta G_c(T,P)}{kT}\right) exp\left(\frac{\Delta F_{diff}(T,P)}{kT}\right)$$

Marcolli, 2020

Parameterizations of ice nucleation rates

Murray et al., 2010, n = 0.97
Murray et al., 2010, n = 0.3
Ickes et al., 2015

- · - · -50 MPa
—— 0.1 MPa
- - - 50 MPa

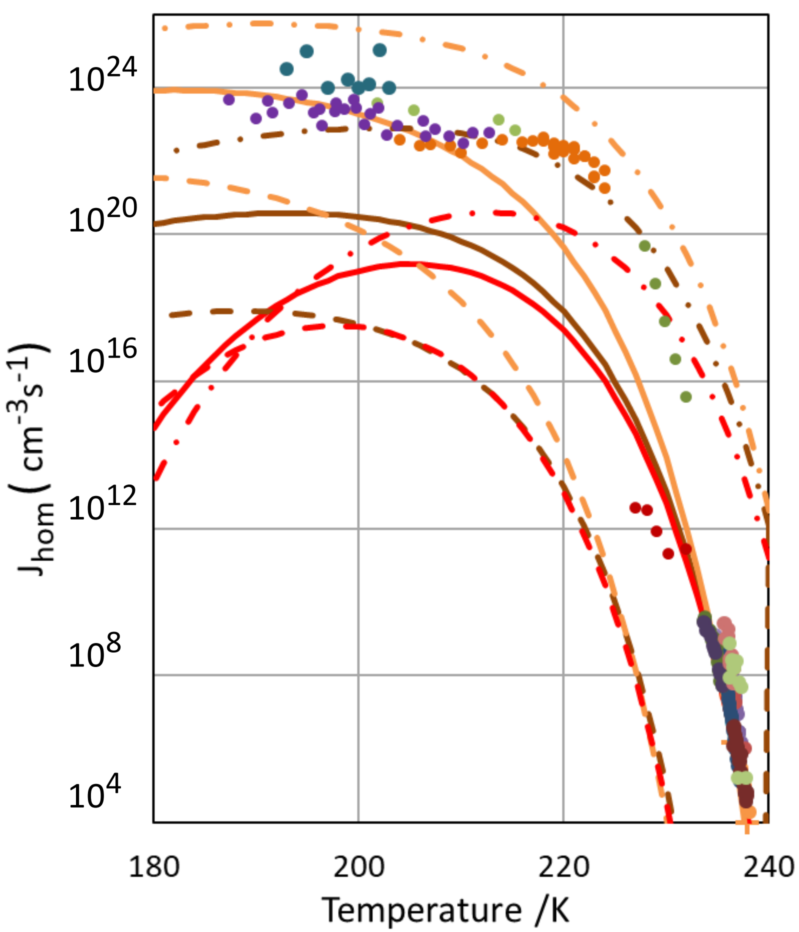

Parameterizations of ice nucleation rates

Young-Laplace equation

$$\Delta P = P - P_0 = \frac{2\gamma_{vw}(T)}{r_c}$$

30 – 50 MPa

~17 MPa

Murray et al., 2010, n = 0.97

Murray et al., 2010, n = 0.3

Ickes et al., 2015

-50 MPa (dash-dot)

0.1 MPa (solid)

50 MPa (dashed)

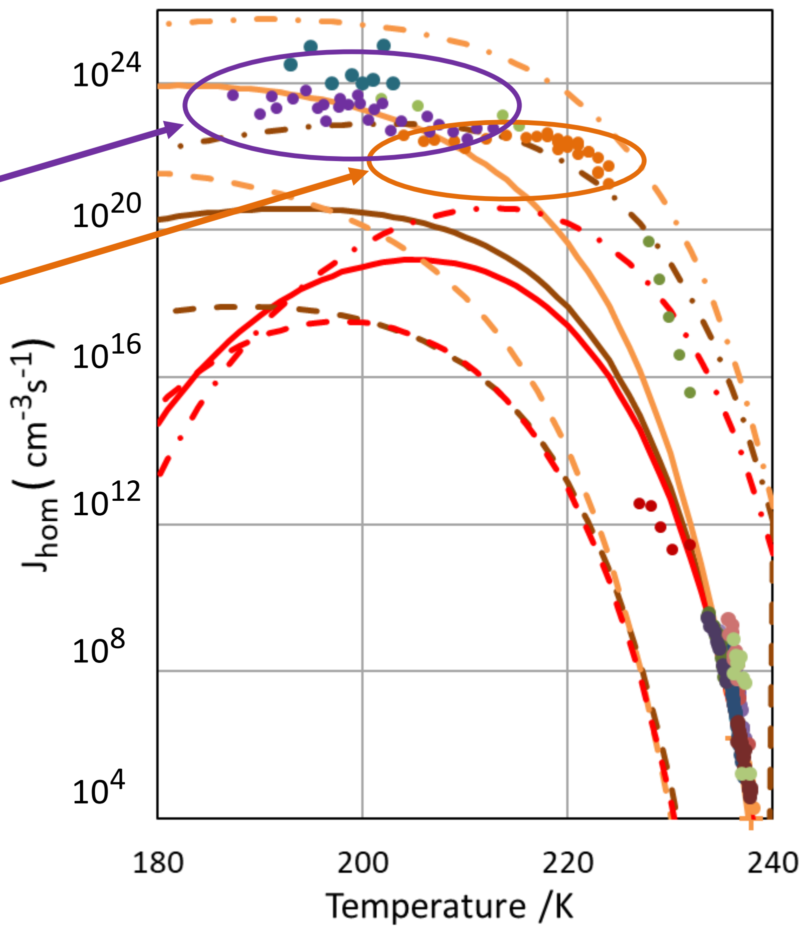

Melting points

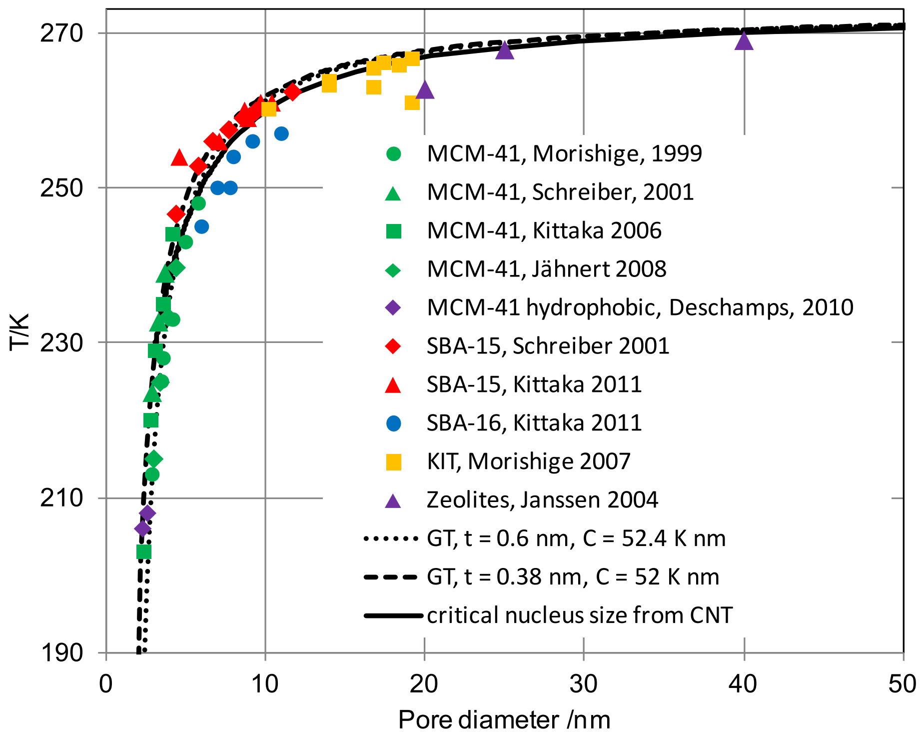

Freezing points

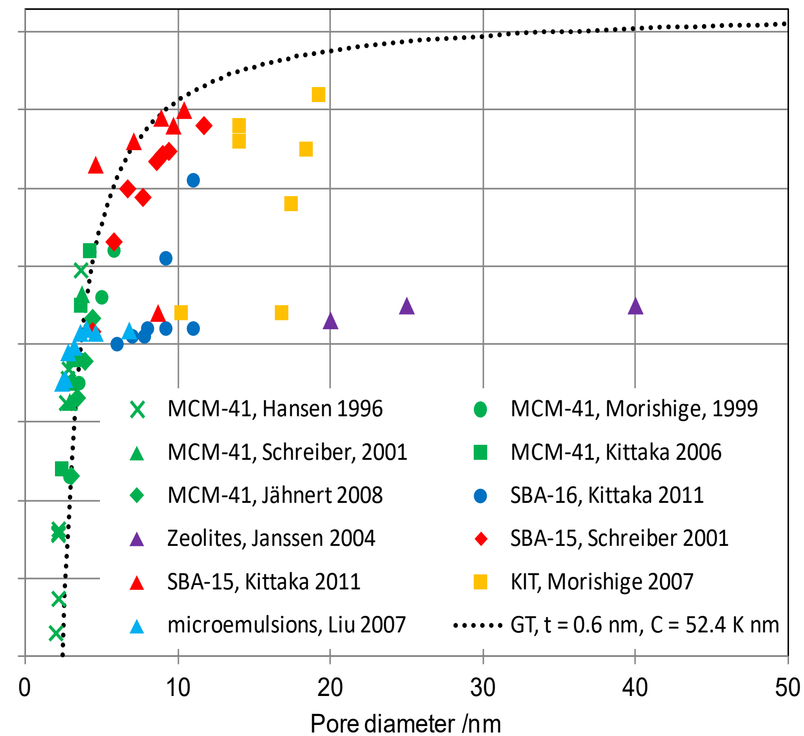

$$r_{crit} = \frac{2\gamma_{iw}(T)v_i}{kT\ln\frac{p_w}{p_i}}$$

Marcolli, 2014

Critical pore size to avoid ice melting in pores

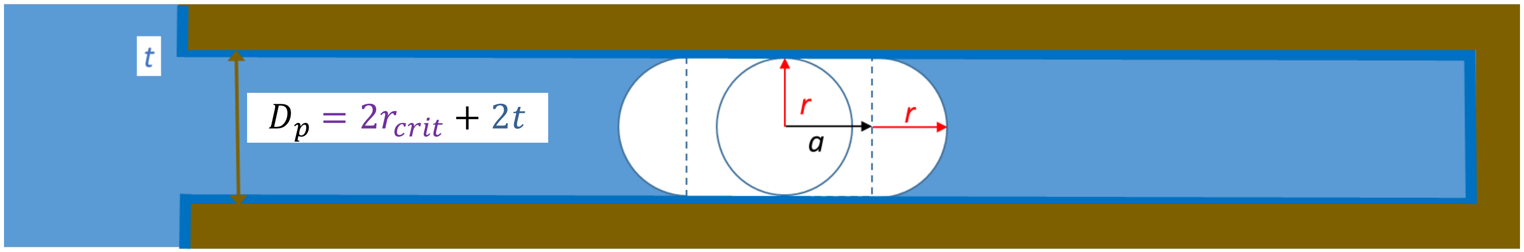

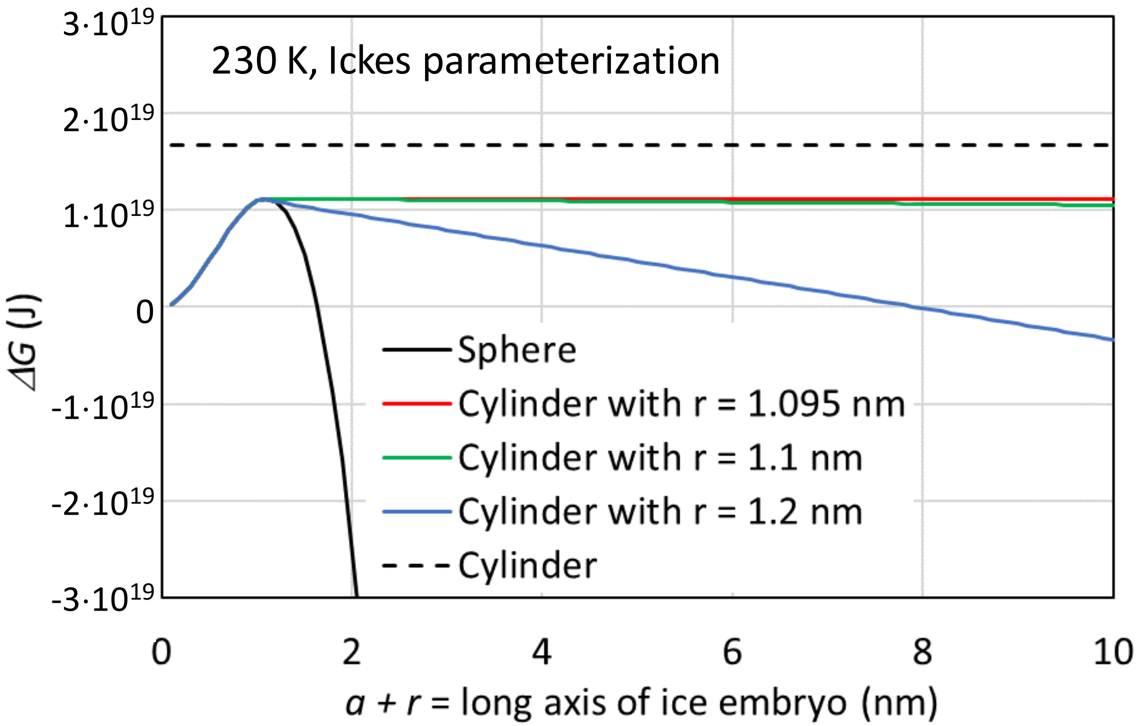

Critical radius from classical nucleation theory:

$$r_{crit} = \frac{2\gamma_{iw}(T)v_i}{kT\ln\frac{p_w}{p_i}}$$

For r_{crit} = 1.095 nm, pore ice remains critical.

For r = 1.1 nm, ice becomes stable at a pore length of 300 nm.

For r = 1.2 nm, ice becomes stable at a pore length of 8 nm.

Marcolli, 2020

Ice-liquid oscillations in nanoconfined water

mW water confined between two nanoscopic disks: coexistence in time because of non-negligible cost of the water-ice interface

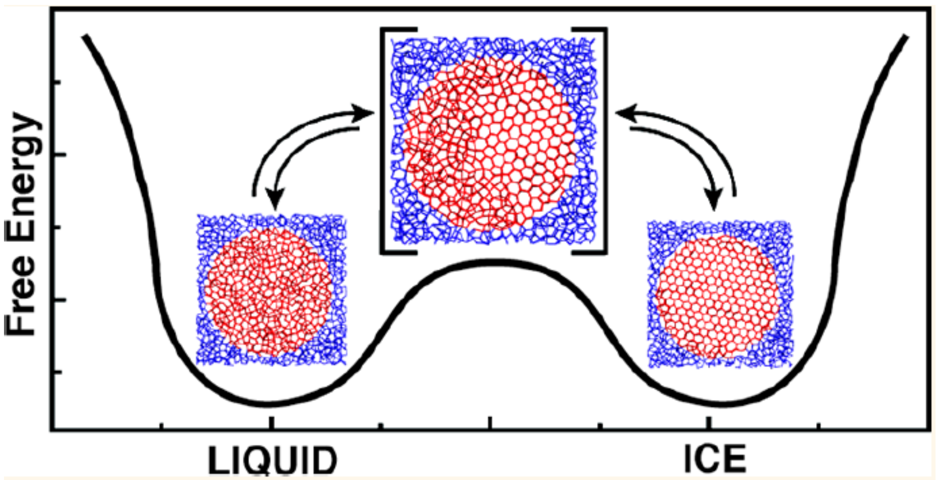

Oscillations between liquid water and ice: free energy profile has two minima, one for all liquid and one for all ice.

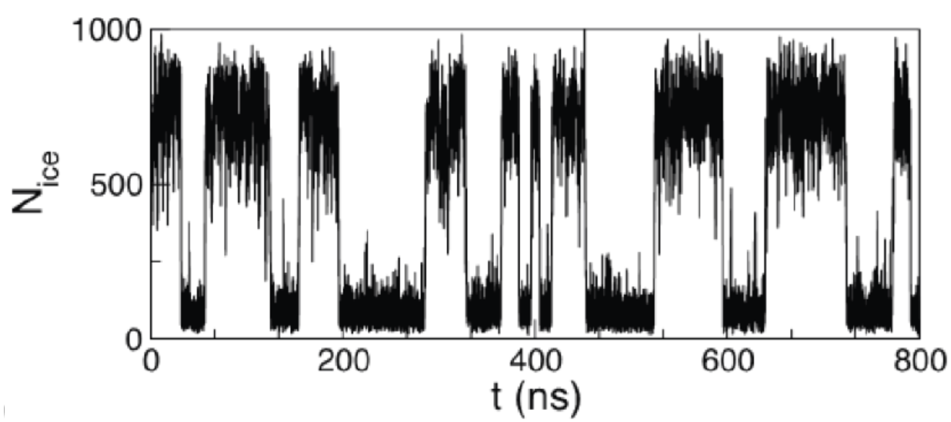

Number of confined water molecules in the ice phase as a function of time at 278.75 K

Kastelowitz and Molinero, 2018

Influence of tension (negative pressure) within the pore

The tension exerted on pore water depends on the radius of curvature as given by the Young-Laplace equation

$$\Delta P = P - P_0 = \frac{2\gamma_{vw}(T)}{r_c}$$

The radius of curvature depends on the water saturation ratio as given by Kelvin equation

$$r_c = \frac{2\gamma_{vw}(T)v_w}{kT\ln\frac{p}{p_w}}$$

Radius of critical embryo depends on pressure

$$r_{crit} = \frac{2\gamma_{wi}(T)v_i(T,P_0)}{kT\ln\frac{p_w}{p_i} - (P-P_0)v_i + (P-P_0)\frac{v_w(T,P)+v_w(T,P_0)}{2}}$$

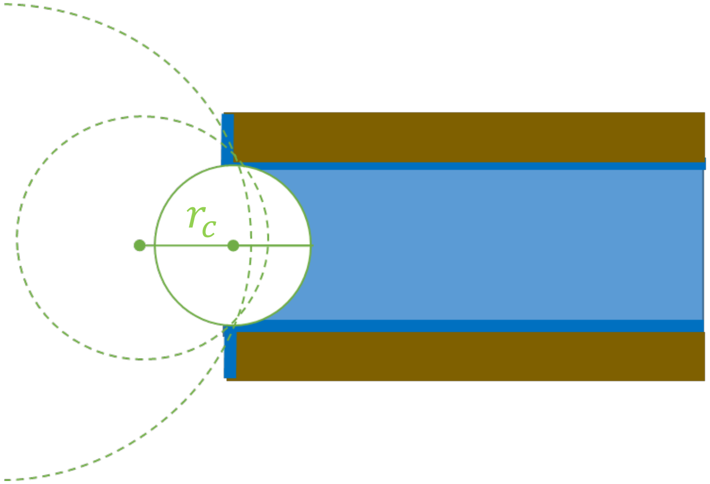

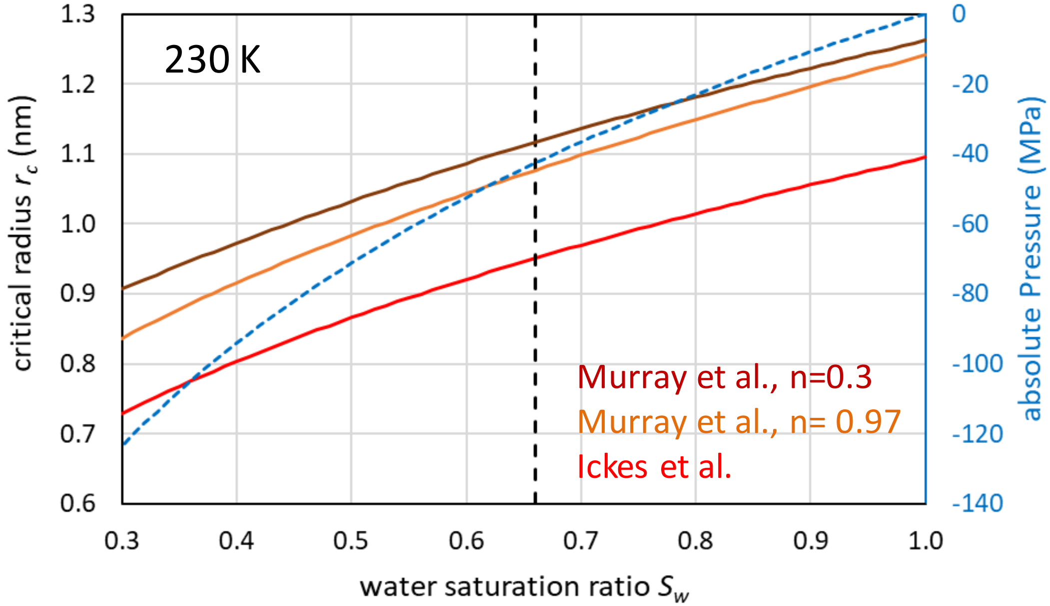

Nucleation rates as a function of pressure and temperature

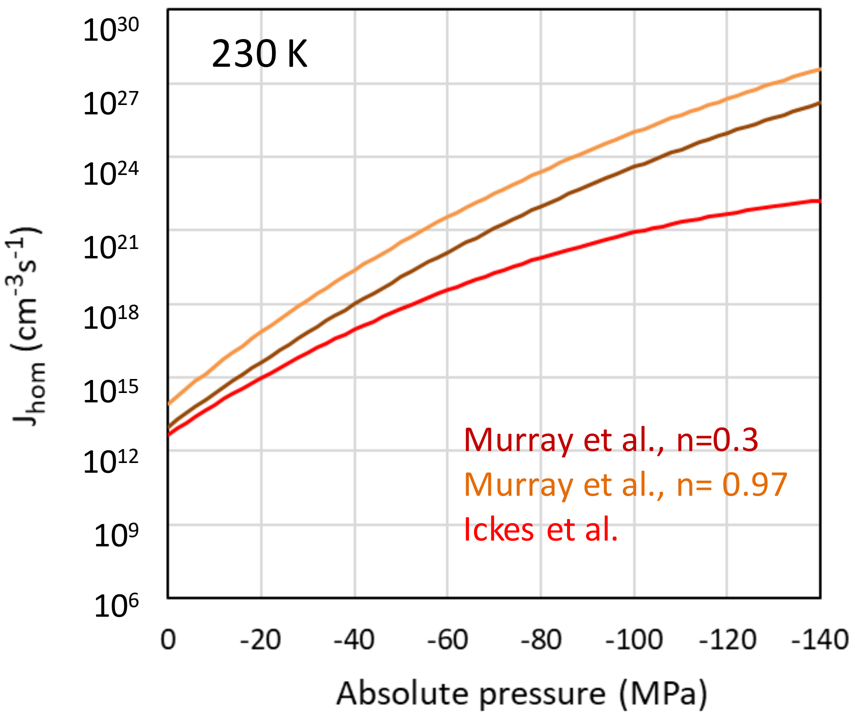

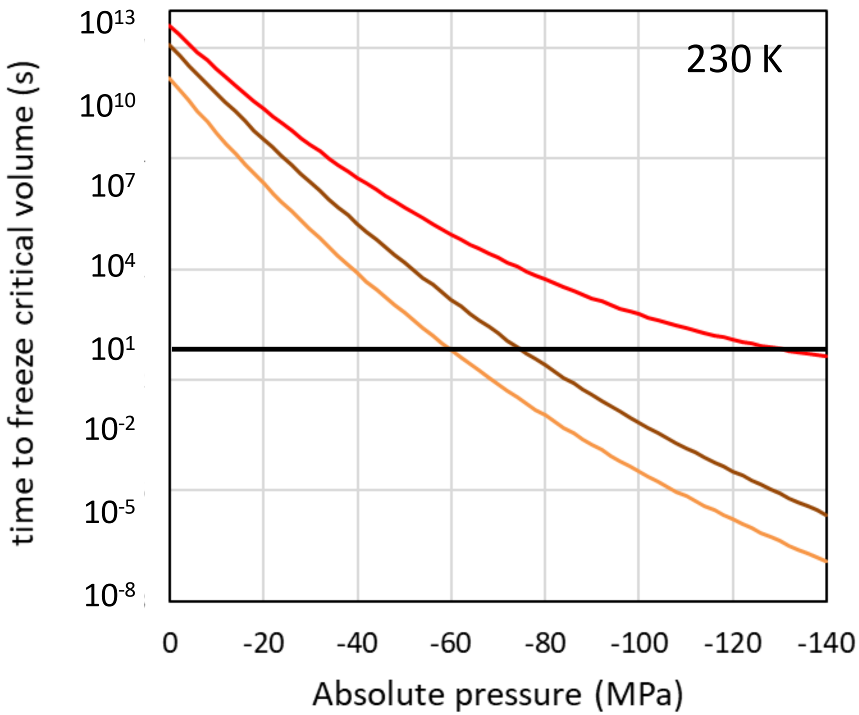

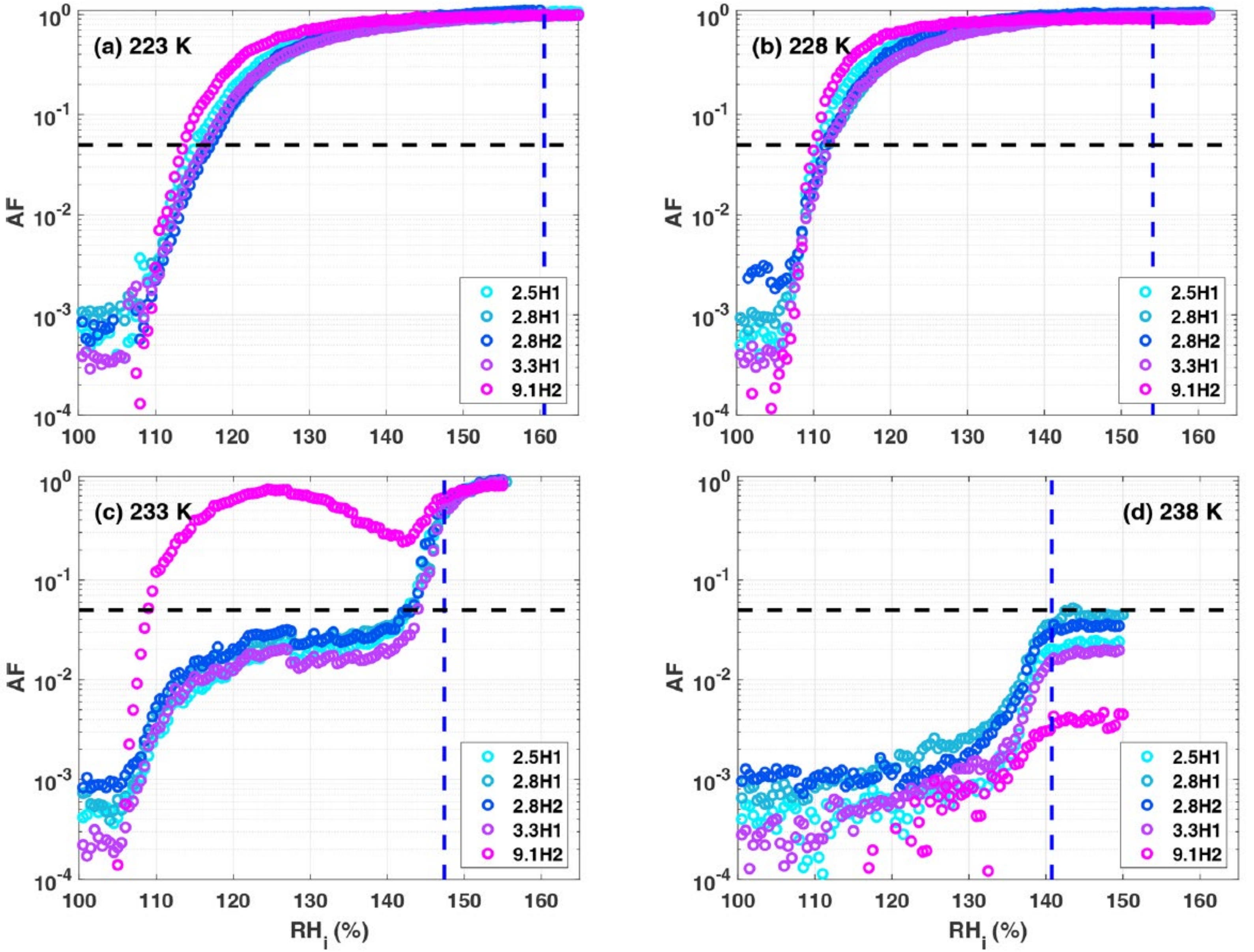

David et al., 2020

Pore condensation and freezing (PCF): ice growth

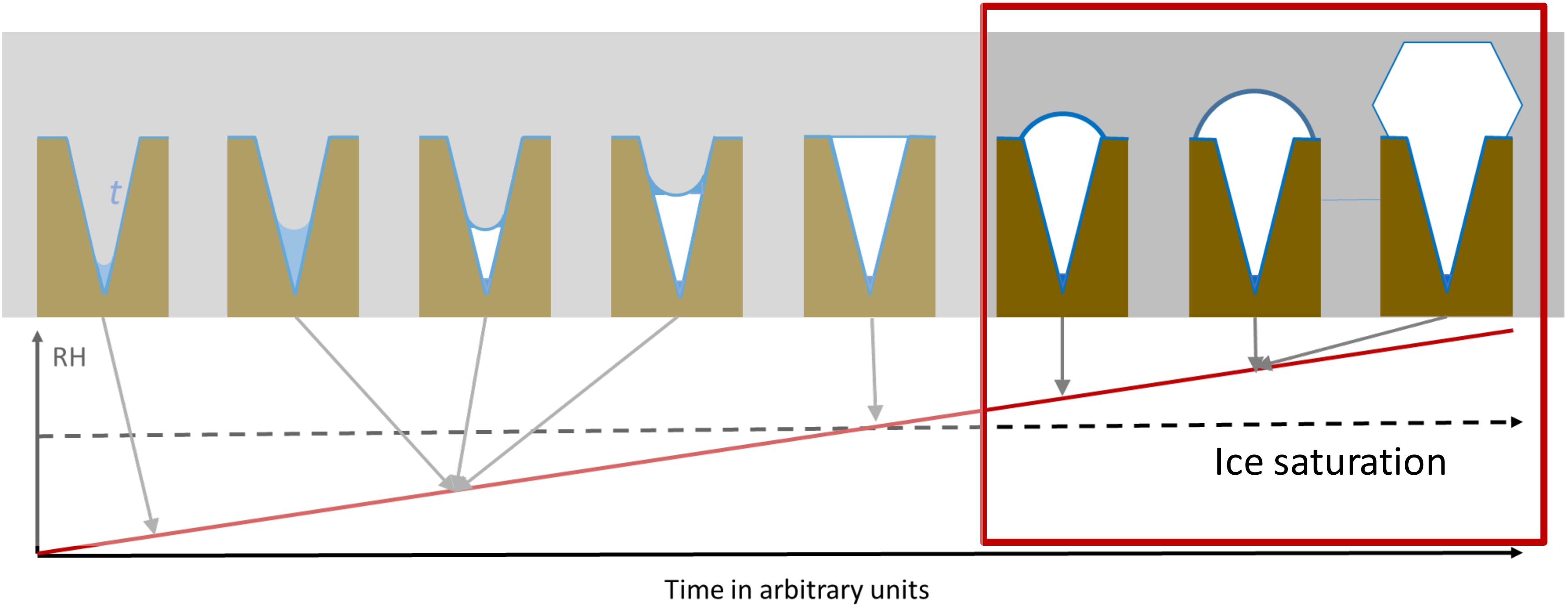

Pore diameter required for growth of ice out of pores

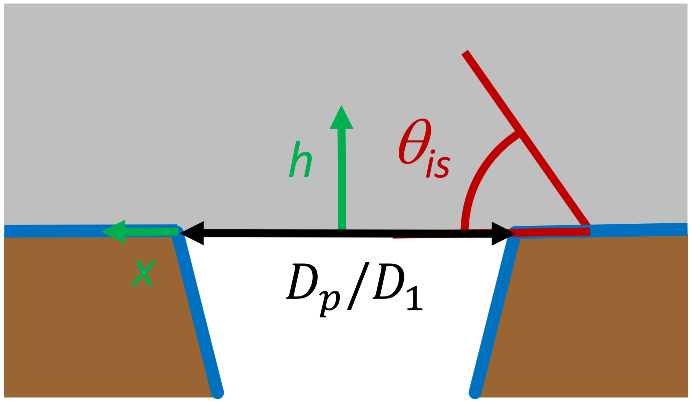

1. Growth of ice in height *h* as spherical cap up to a contact angle θ_{is}

2. Growth of the cap base (increase in *x*)

Assumption: water wets particle surface

$\theta_{is} = \theta_{iw} \approx 55°$

$$\cos\theta_{iw}(T) = \frac{\gamma_{vw}(T) - \gamma_{iw}(T, P_0)}{\gamma_{vi}(T)}$$

Conical pore $\quad D_p = \dfrac{4\gamma_{vi} v_i \sin\theta_{iw}}{kT\ln\frac{p}{p_{ih}}}$

Wedge-shaped pore $\quad D_1 = \dfrac{2\gamma_{vi} v_i \sin\theta_{iw}}{kT\ln\frac{p}{p_{ih}}}$

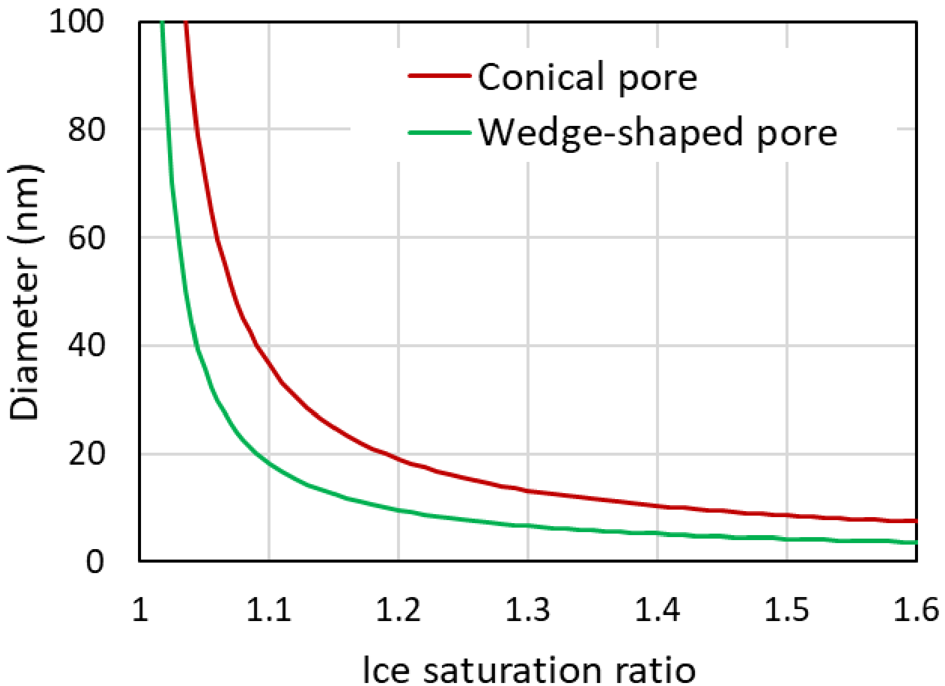

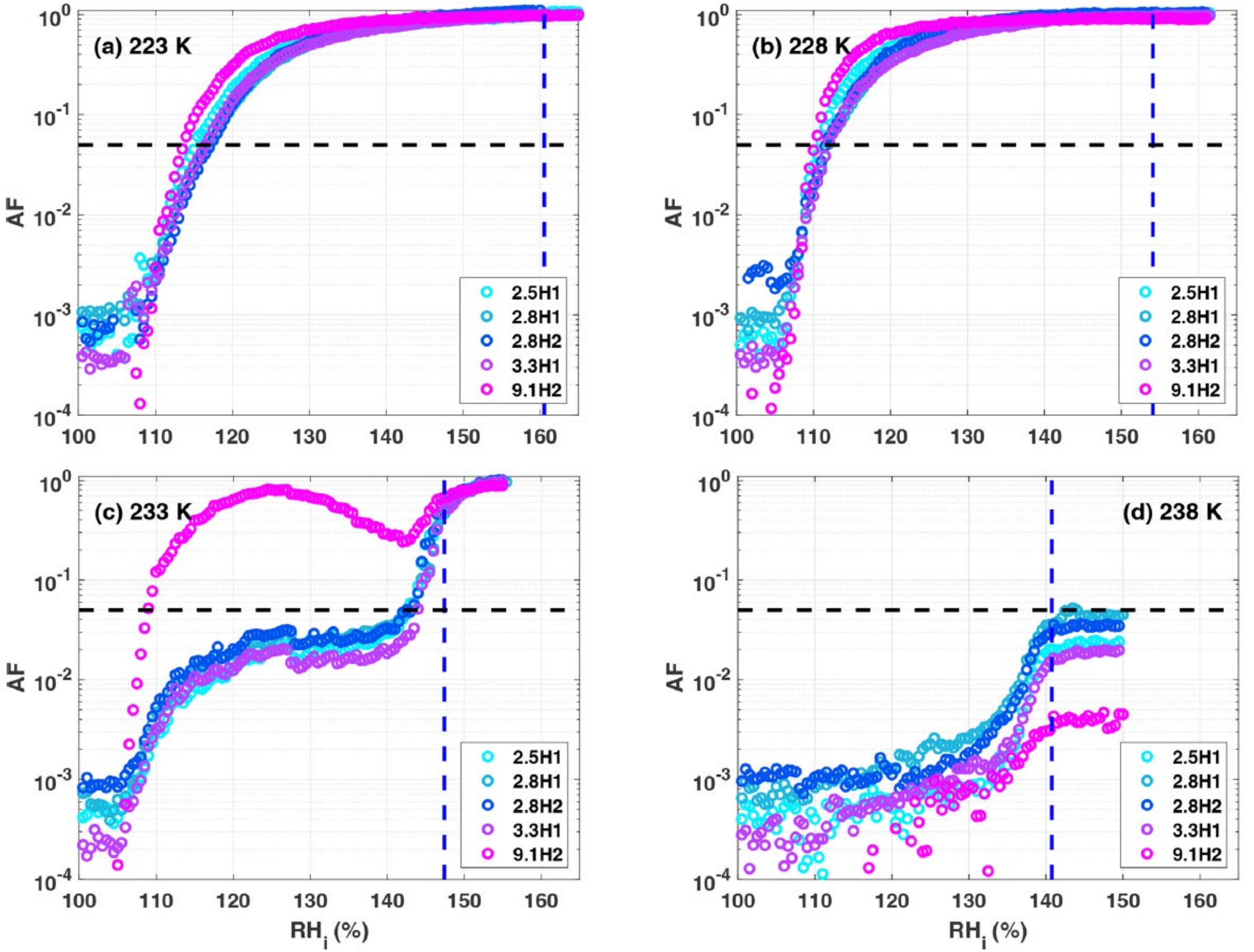

David et al., 2020

MD simulations of ice growth out of pores

Molecular dynamics simulations with the mW model:

- Dimensions of the periodic simulation cells are 8 nm × 8 nm × 10 nm
- The pore and outer surface represent silica properties (grey).
- 3 nm diameter pores are filled with hexagonal ice exposing the primary prismatic face to vapor.
- Liquid water (red) and ice (blue) are identified using the CHILL+ algorithm.
- The vapor uptake is performed at −81°C with RH_i = 250 %.

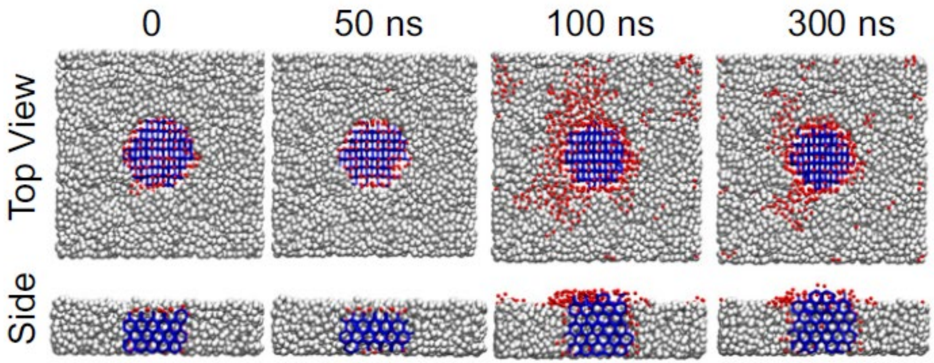

David et al., 2019

MD simulations of ice growth out of pores

Molecular dynamics simulations with the mW model:

– Dimensions of the periodic simulation cells are 8 nm × 8 nm × 10 nm
– The pore and outer surface represent silica properties (grey).
– 3 nm diameter pores are filled with hexagonal ice exposing the primary prismatic face to vapor.
– Liquid water (red) and ice (blue) are identified using the CHILL+ algorithm.
– The vapor uptake is performed at −81 °C with RHi = 250%.

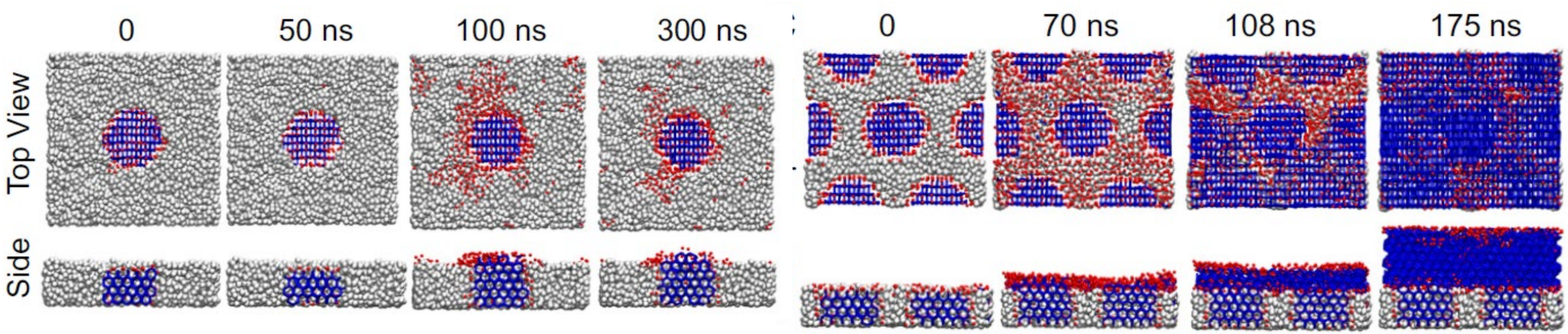

Pore ice bridging allows growth of ice out of pores:

Water condenses between emerging pore ice and freezes leading to an ice surface for further growth.

David et al., 2019

Pore diameter required for growth of ice out of pores

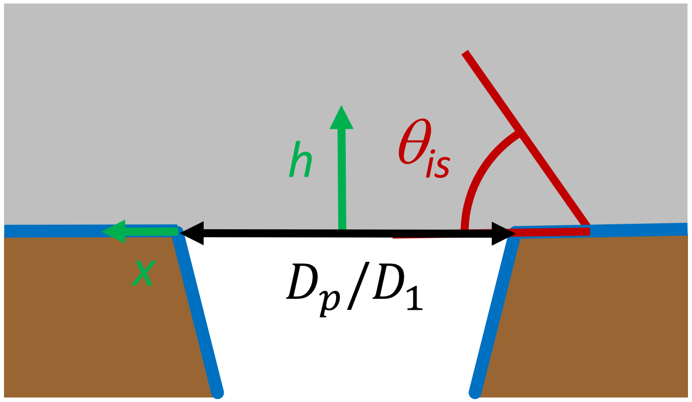

Conical pore $D_p = \dfrac{4\gamma_{vi} v_i sin\theta_{iw}}{kTln\dfrac{p}{p_{ih}}}$

Wedge-shaped pore $D_1 = \dfrac{2\gamma_{vi} v_i sin\theta_{iw}}{kTln\dfrac{p}{p_{ih}}}$

1. Growth of ice in height *h* as spherical cap up to a contact angle θ_{is}

2. Growth of the cap base (increase in *x*)

Assumption: water wets particle surface

$\theta_{is} = \theta_{iw} \approx 55°$

$$cos\theta_{iw}(T) = \frac{\gamma_{vw}(T) - \gamma_{iw}(T, P_0)}{\gamma_{vi}(T)}$$

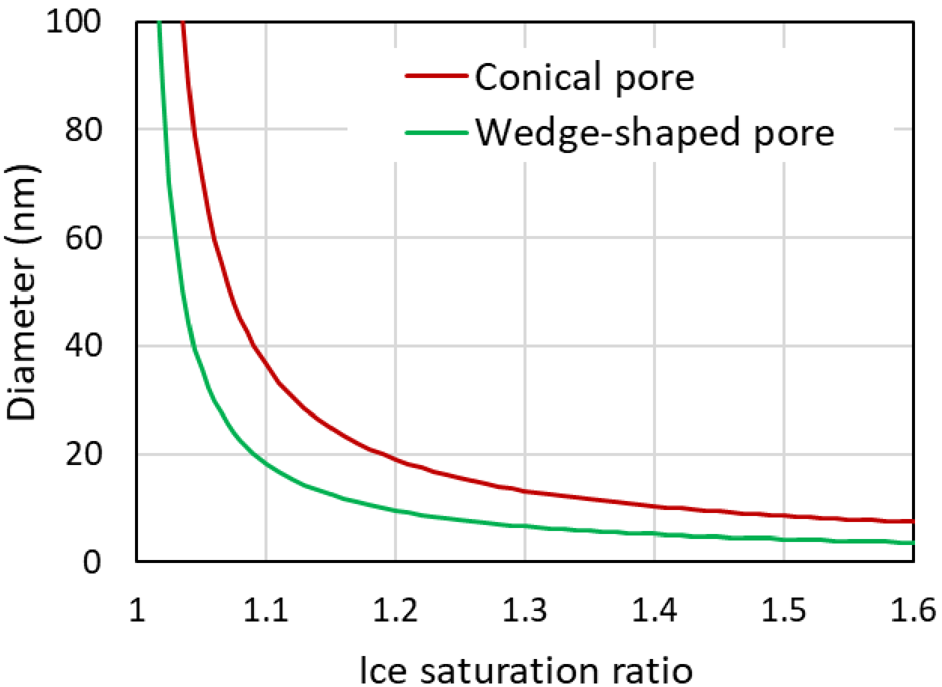

Ice nucleation data for soot

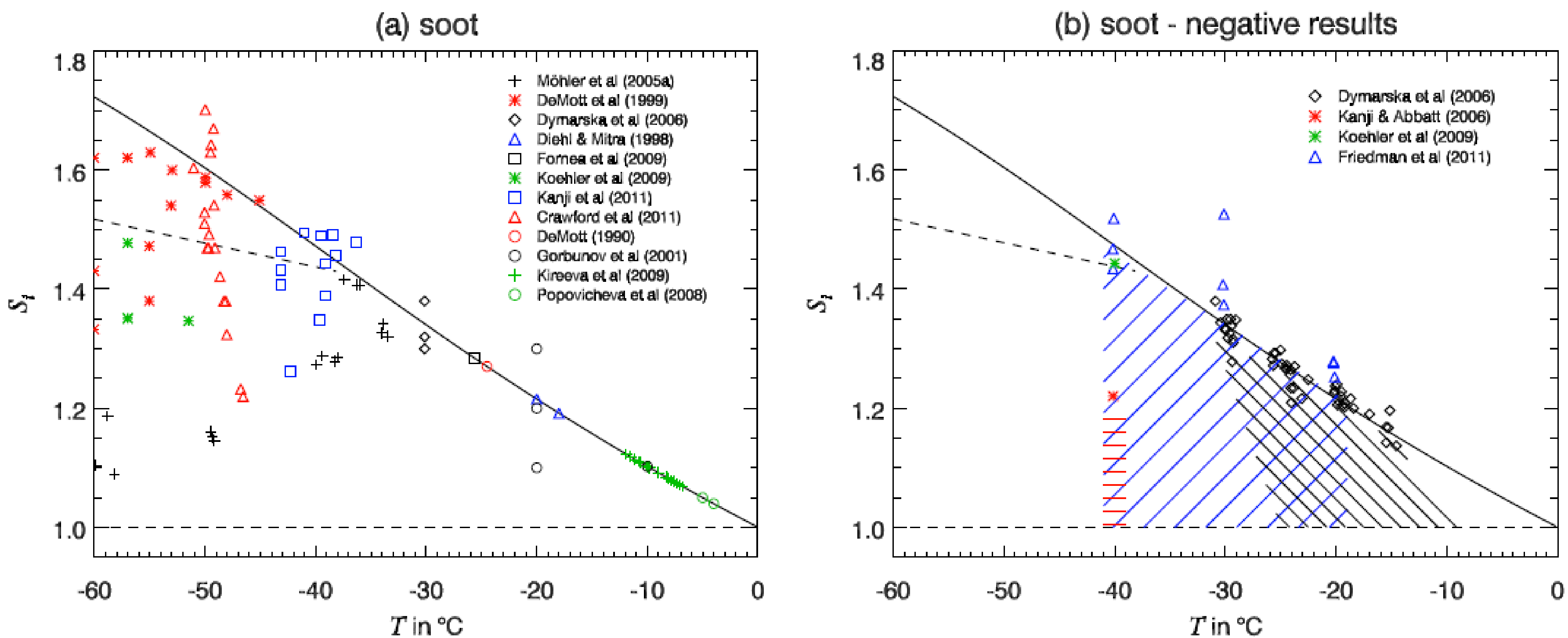

Characteristics for PCF:

– No ice nucleation below water saturation above the homogeneous ice nucleation temperature

– Ice nucleation below water saturation below the homogneous ice nucleation temperature

What is the pore geometry?

Hoose and Möhler, 2012

Morphology of atmospheric soot particles

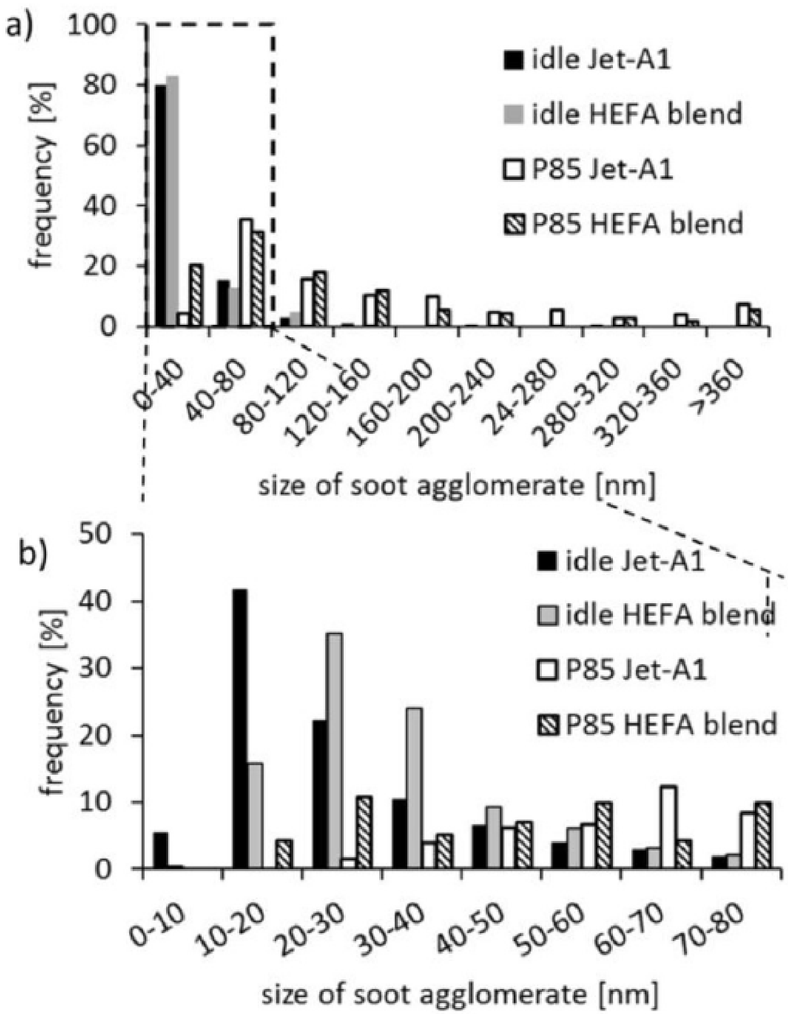

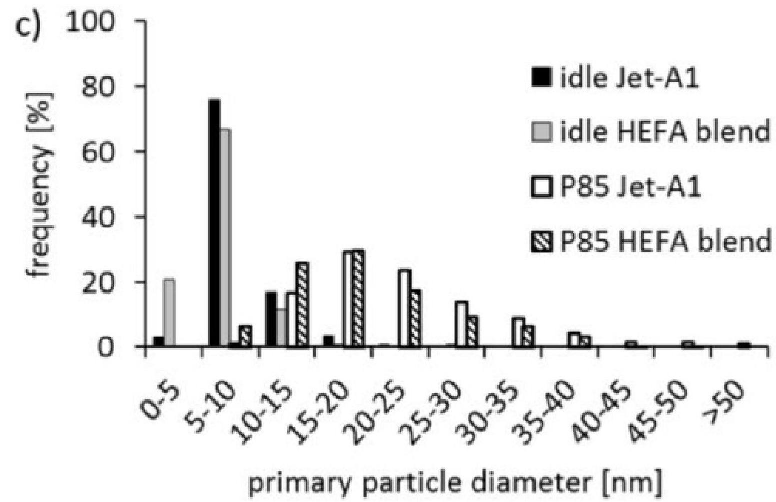

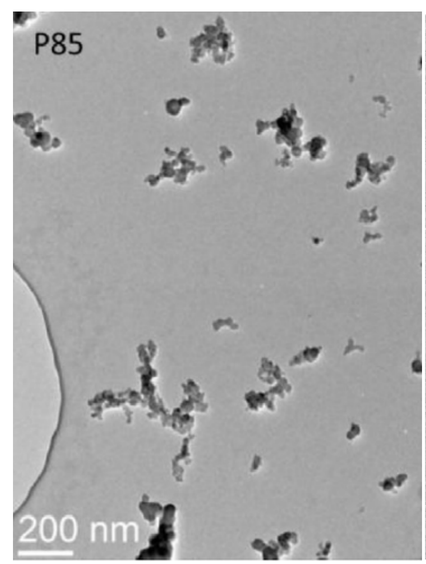

Liati et al., 2019

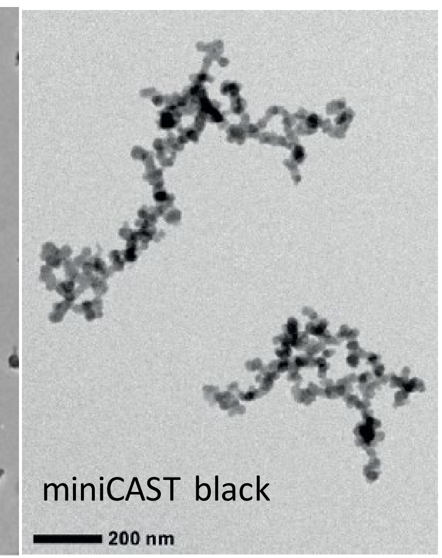

Mahrt et al., 2018

Pores within soot aggregates

Tetrahedral packing
26.0 % free space

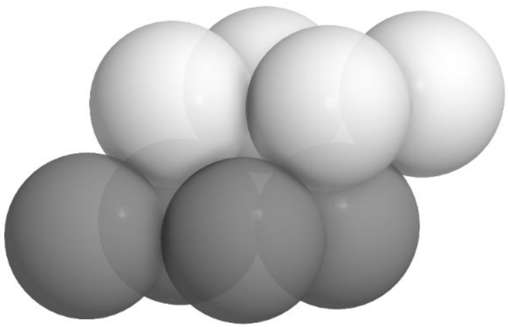

Three-membered ring pore

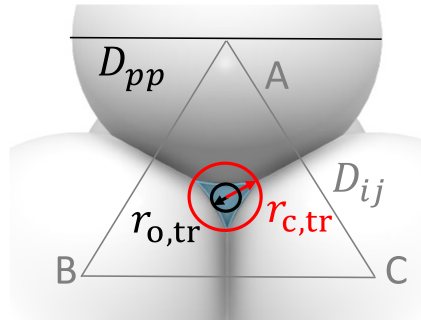

Concave octahedron

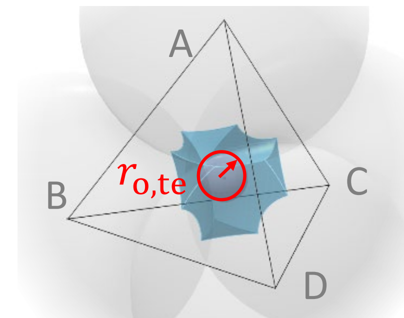

Cubic packing
47.6 % free space

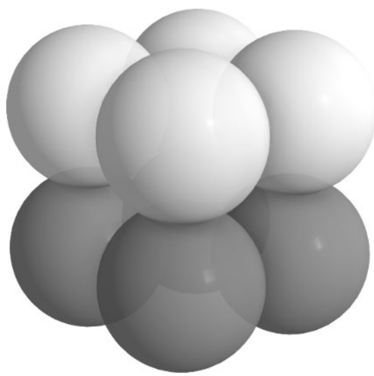

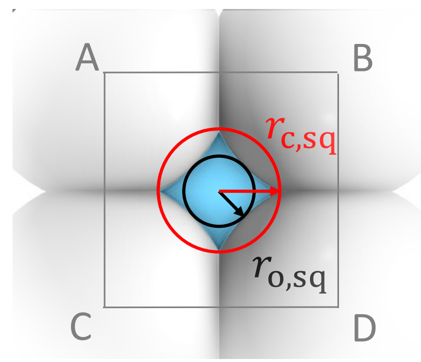

Four-membered ring pore

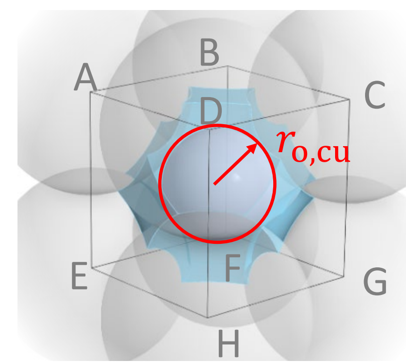

Concave cube

Spherical primary particles with typical diameters D_{pp} = 10–30 nm

Overlap $C_{ov} = \frac{D_{pp} - D_{ij}}{D_{pp}}$ = 0.01–0.2

Ring pore sizes for primary particle diameters from 10 to 30 nm

Three-membered ring pore

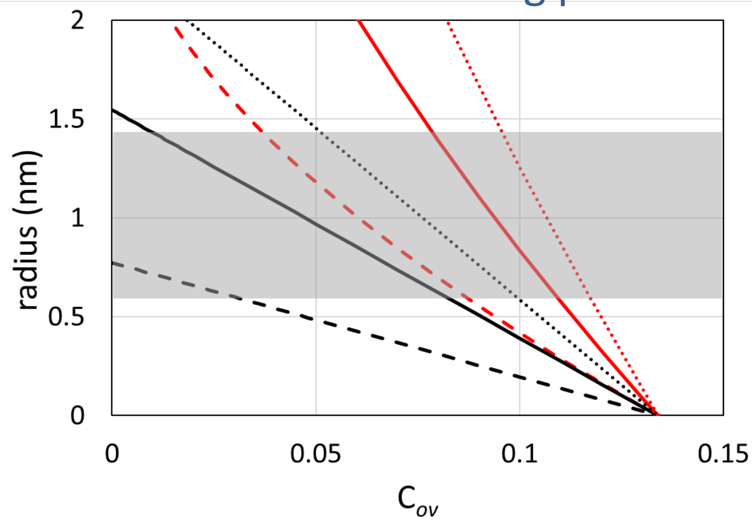

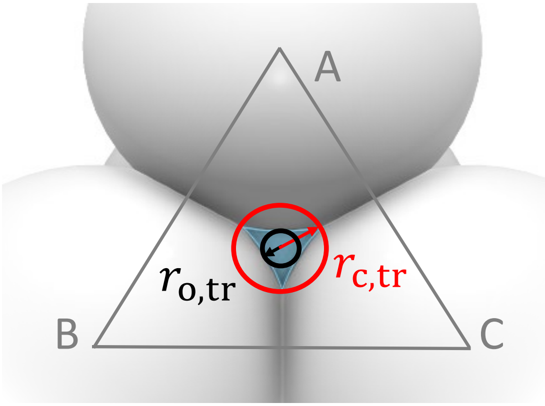

Four-membered ring pore

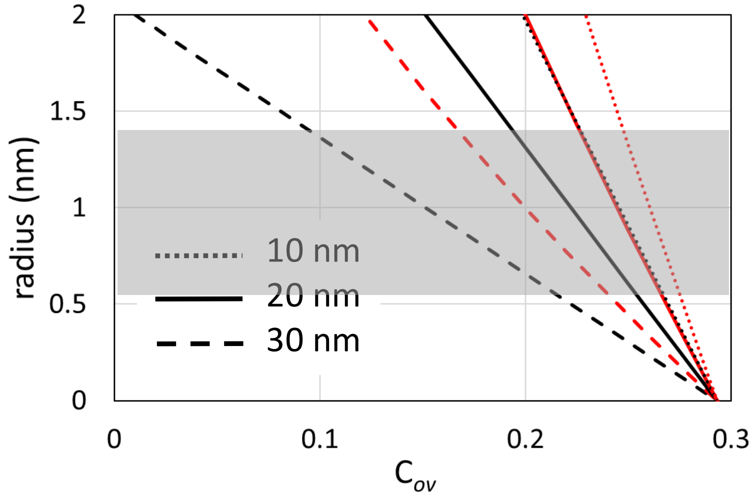

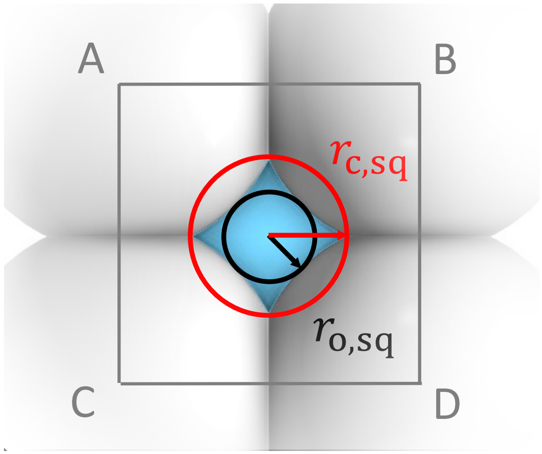

Soot-PCF: primary particle diameter: 20 nm, C_{ov} = 0.05

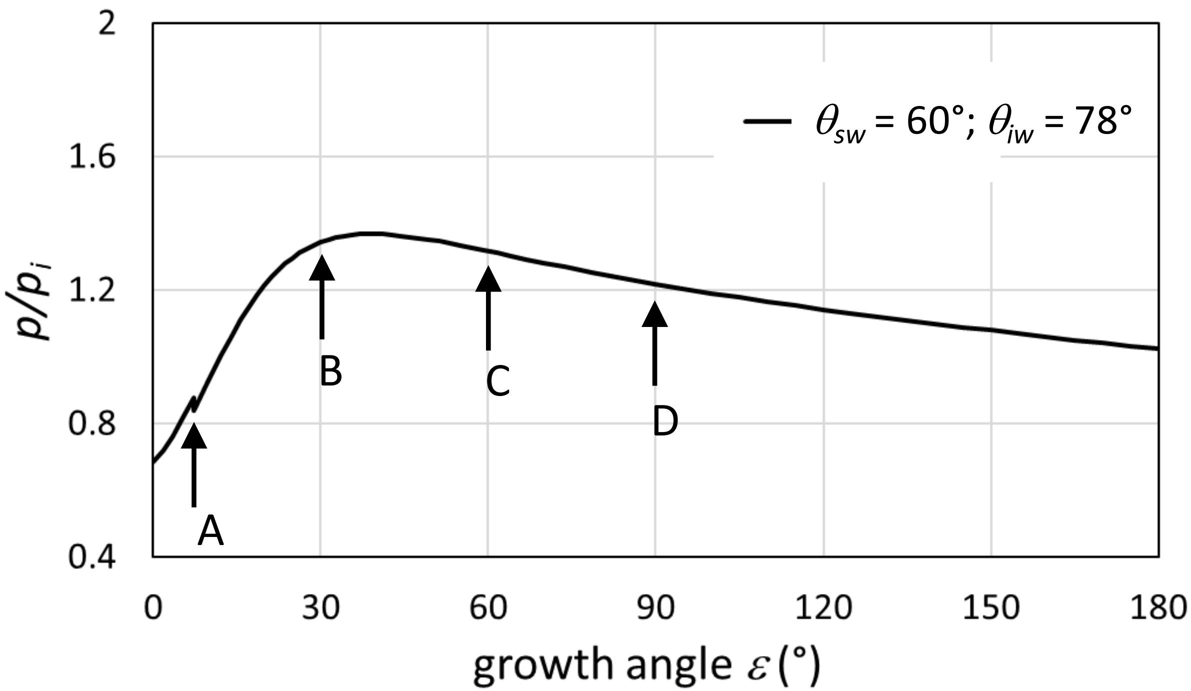

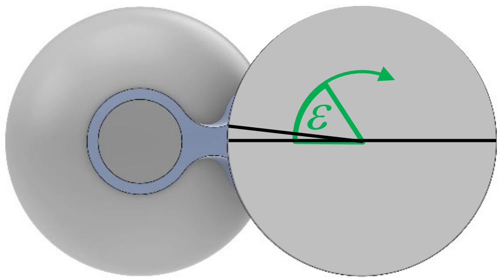

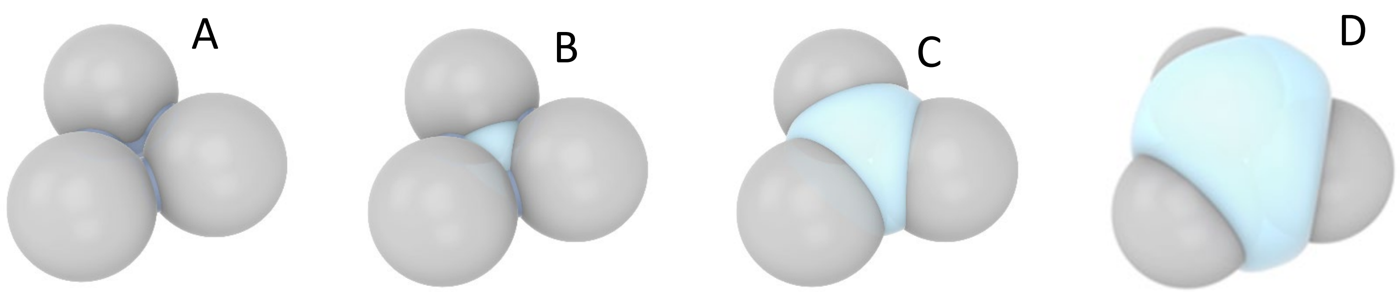

Soot-PCF: primary particle diameter: 20 nm, C_{ov} = 0.05

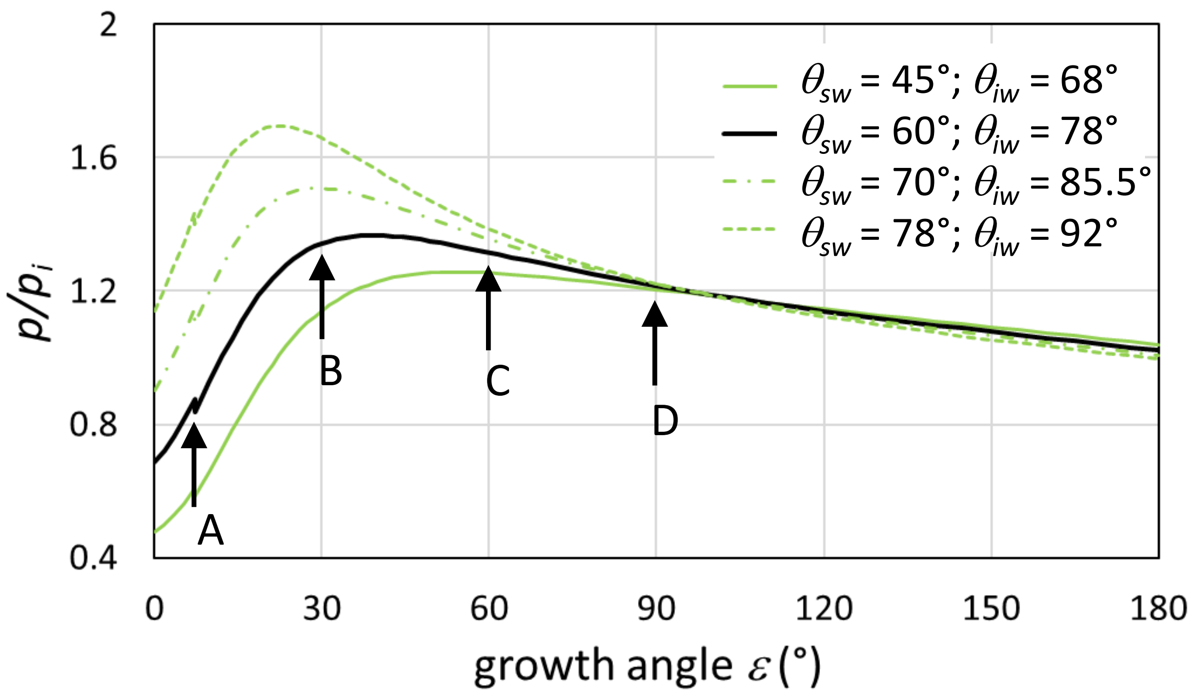

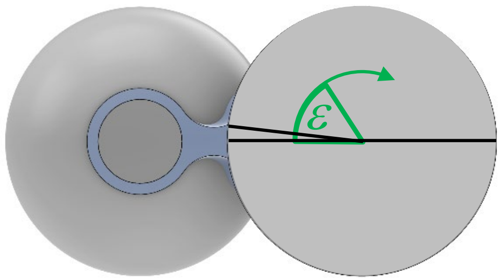

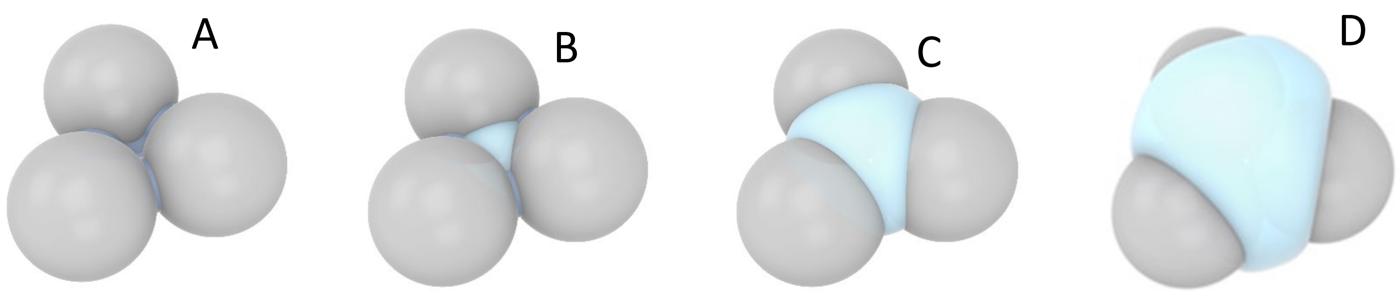

Soot-PCF: primary particle diameter: 20 nm, C_{ov} = 0.1

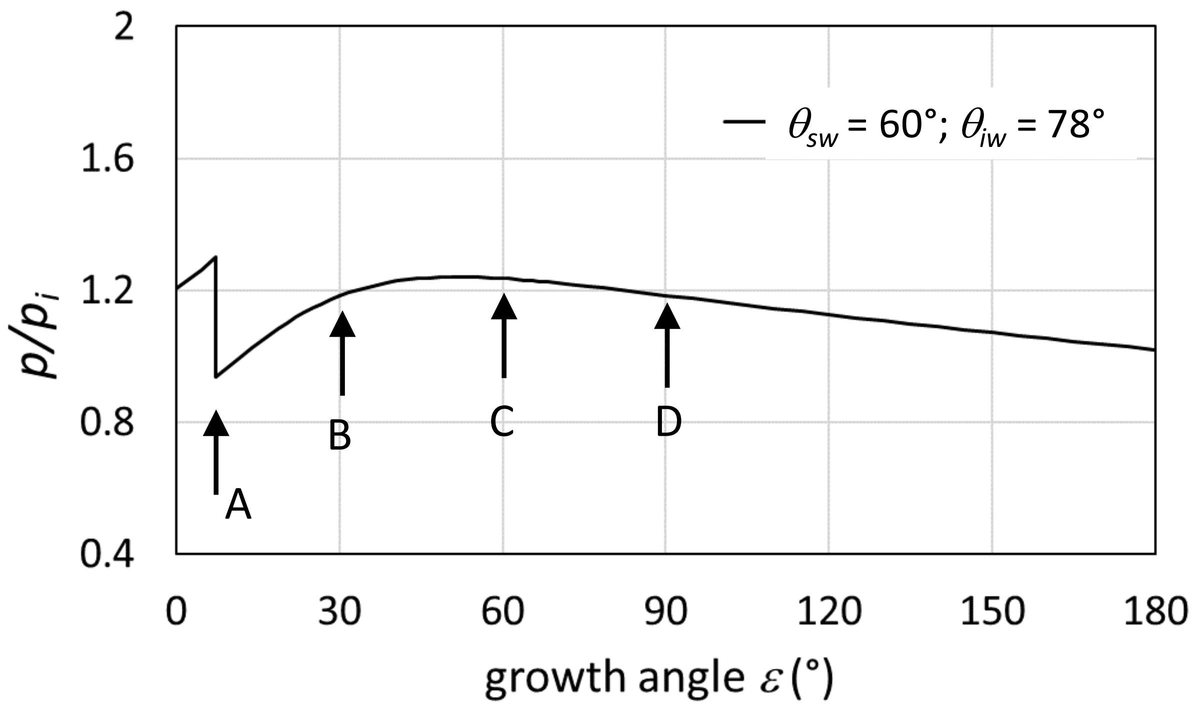

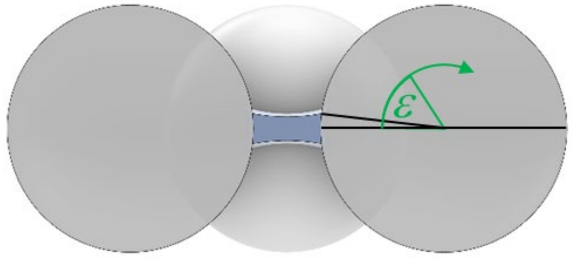

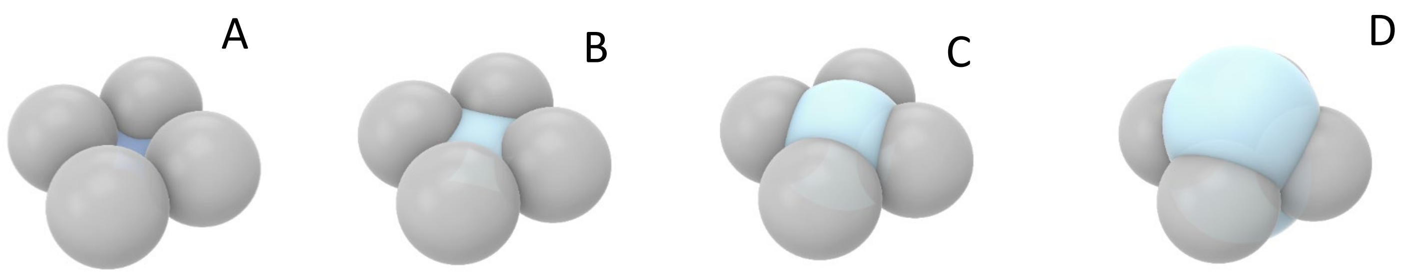

Soot-PCF: primary particle diameter: 20 nm, C_{ov} = 0.1

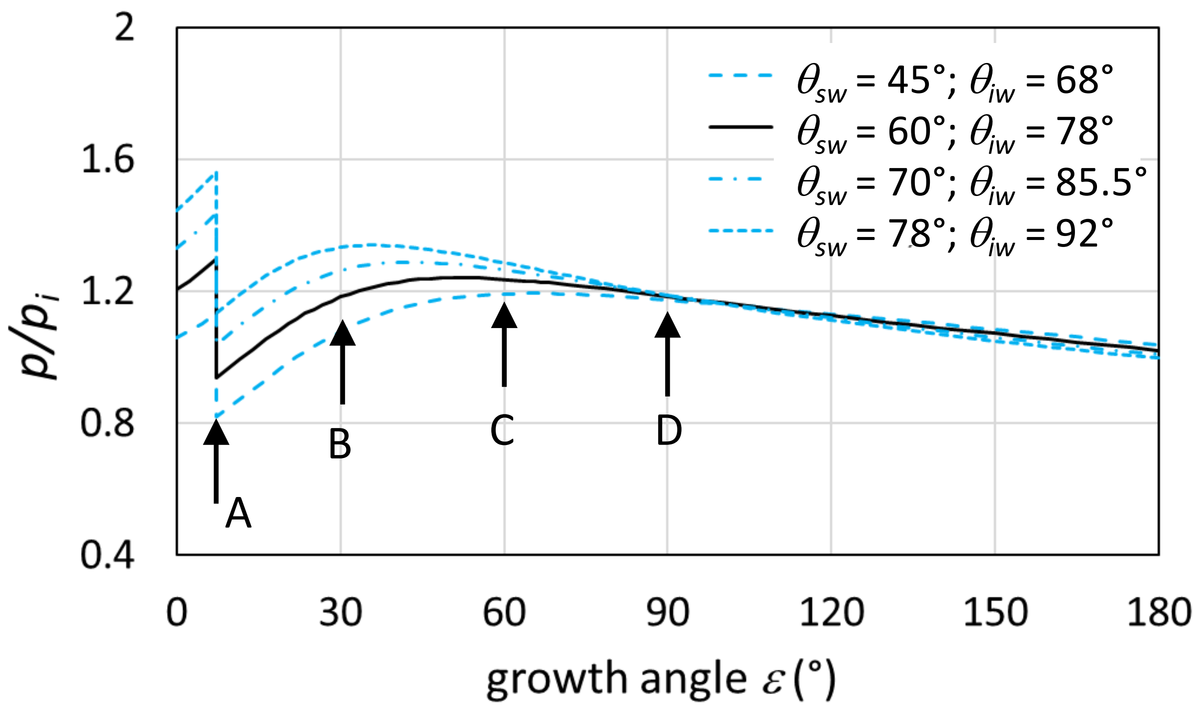

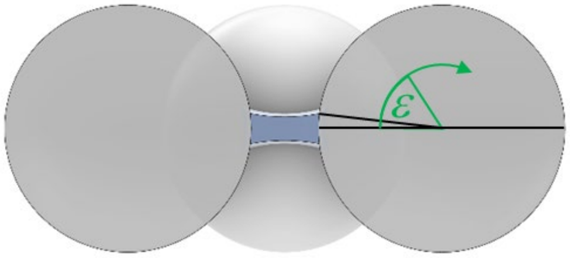

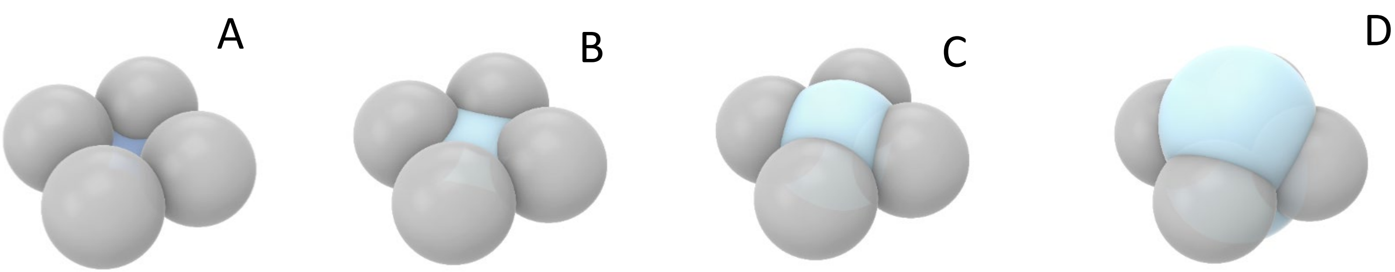

Parameterization of activated fraction (*AF*) realized by ring pores

$$AF = 1 - \left(1 - P_{\mathrm{N}}(RH)\right)^{\left((N_{\mathrm{p}} - n_{\mathrm{m}})^{D_{\mathrm{f}}}\right)}$$

$P_{\mathrm{N}}(RH)$: probability of a primary particle to be part of a ring pore activating at RH. Depends on primary particle size, overlap, and contact angle

n_{m}: accounts of minimum number of primary particles required for a ring pore

D_{f}: fractal dimension accounting for the number of neighbours of a primary particle.

N_{p}: number of primary particles in an aggregate: $N_{\mathrm{p}} = k_0 \left(\frac{2R_{\mathrm{g}}}{D_{\mathrm{pp}}}\right)^{D_{\mathrm{f}}}$

k_0: scaling pre-factor ($k_0 = 1.3 \pm 0.2$)

R_{g}: radius of gyration ($2R_{\mathrm{g}} = \frac{D_{\mathrm{m}}}{\beta}$)

D_{m}: mobility diameter

β: in the single particle limit: $\beta = 1.29$

Instrumental setup

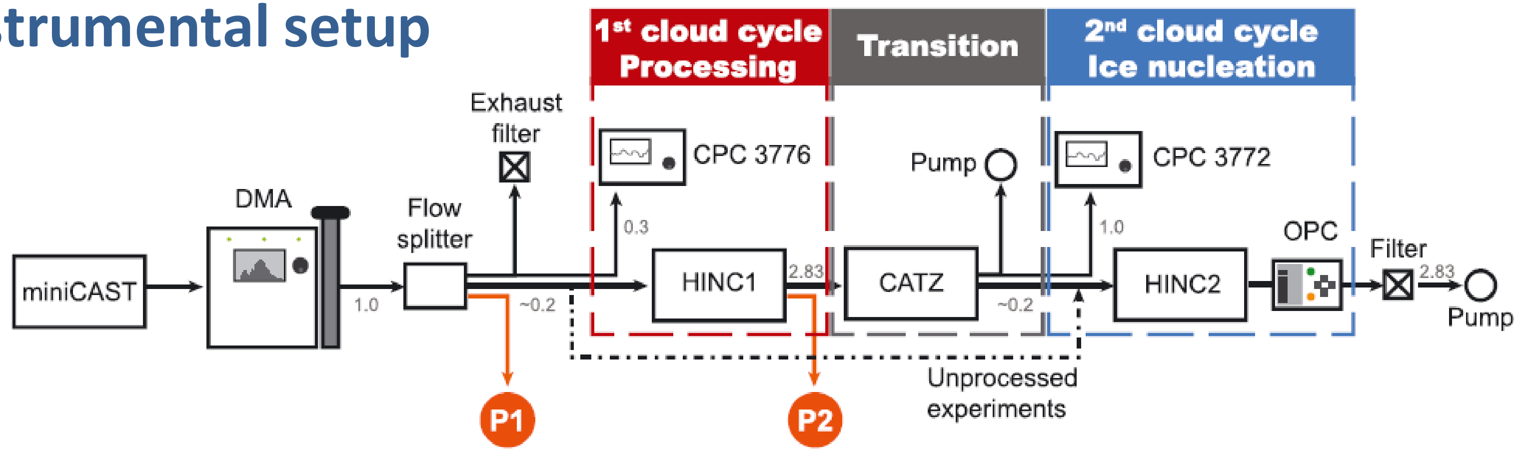

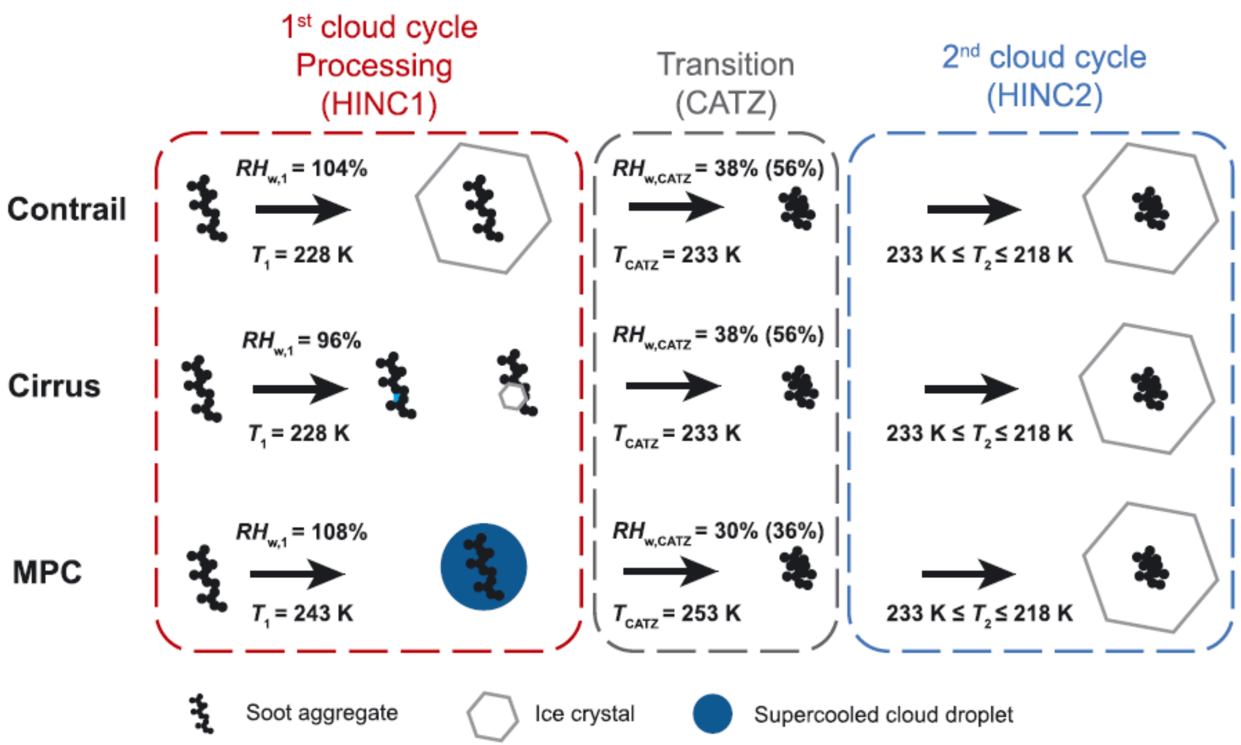

Mahrt et al., 2020

Activated fraction of processed miniCAST black (HINC2)

400 nm diameter

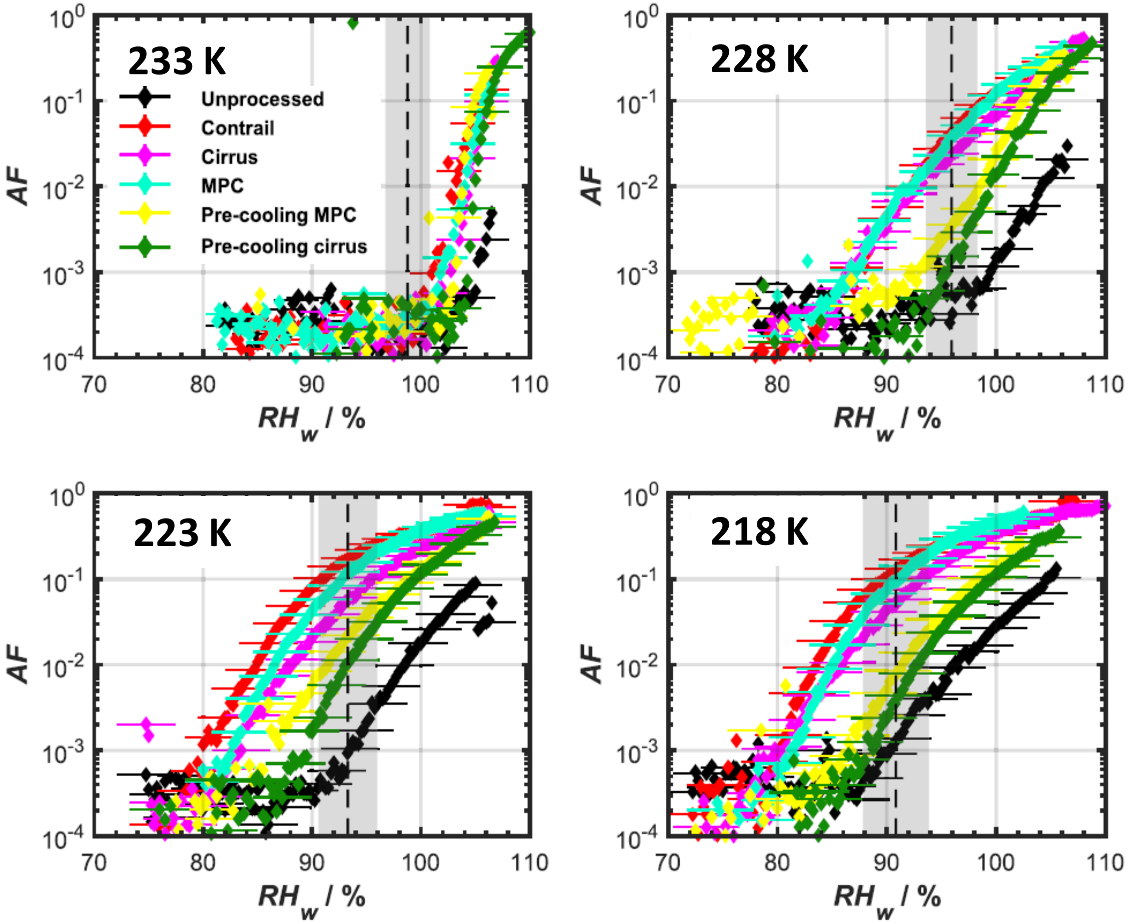

	HINC1	CATZ	HINC2
Unpro-cessed	–	–	70–110 % RH_w 218–233 K
contrail	104 % RH_w 228 K	38 % RH_w 233 K	70–110 % RH_w 218–233 K
cirrus	96 % RH_w 228 K	38 % RH_w 233 K	70–110 % RH_w 218–233 K
MPC	108 % RH_w 243 K	30 % RH_w 253 K	70–110 % RH_w 218–233 K
Precool MPC	96 % RH_w 243 K	30 % RH_w 253 K	70–110 % RH_w 218–233 K
Precool cirrus	65 % RH_w 228 K	38 % RH_w 233 K	70–110 % RH_w 218–233 K

Mahrt et al., 2020

Activated fraction of processed miniCAST black

400 nm diameter

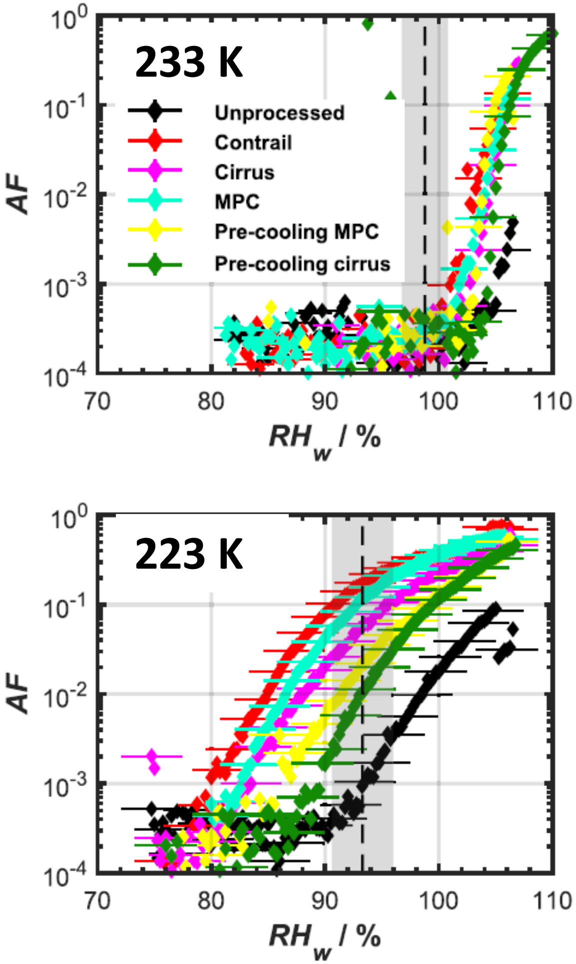

Size dependence

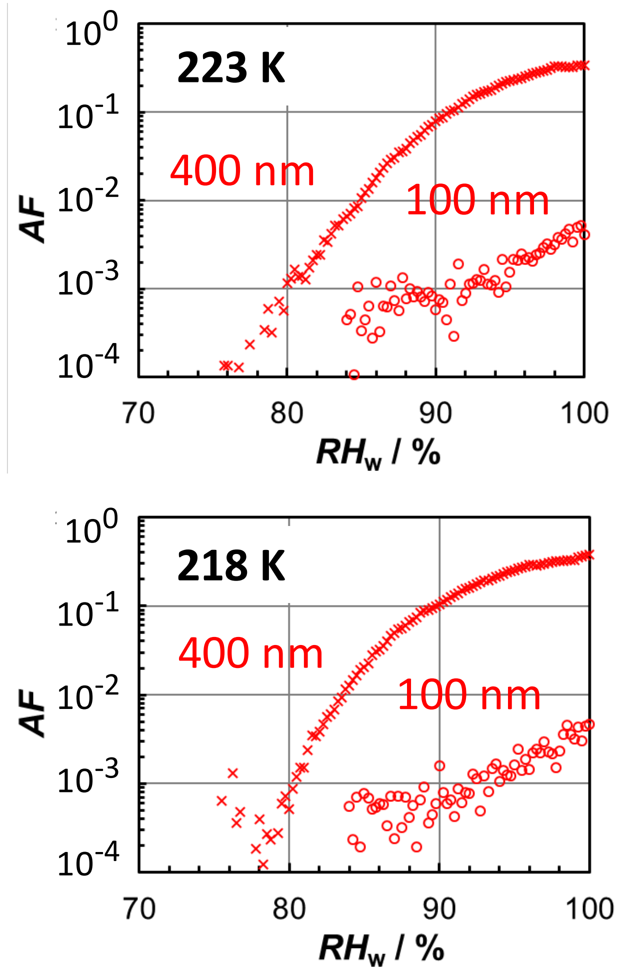

Mahrt et al., 2020

AF parameterization of miniCAST black

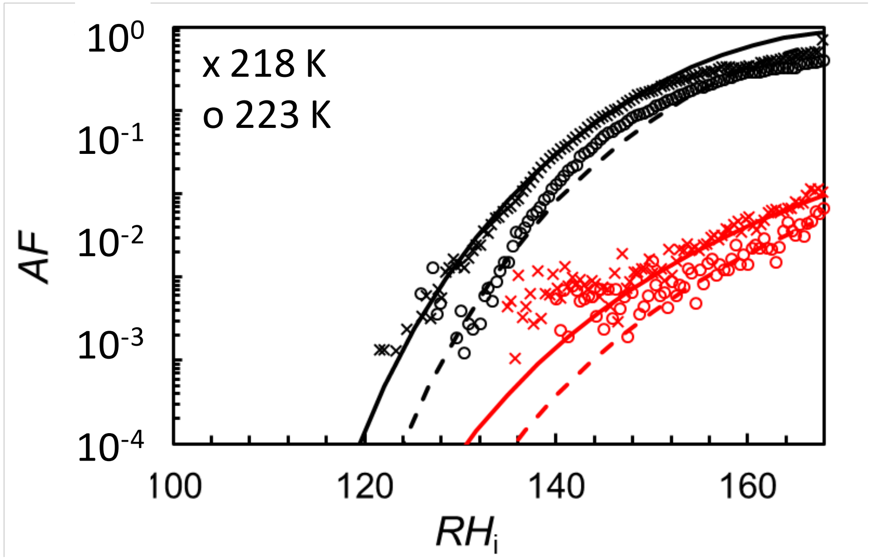

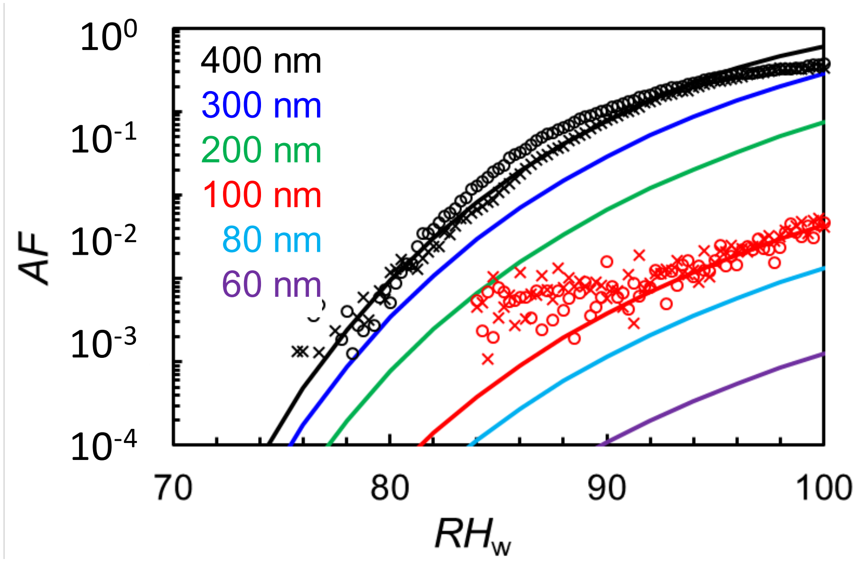

$$AF = 1 - \left(1 - P_{\mathrm{N}}(RH)\right)^{\left((N_{\mathrm{p}}-2)^{1.86}\right)}$$

$$P_{\mathrm{N}}(RH_{\mathrm{w}}) = 10^{\left(\frac{1}{0.3374-0.006091 RH_{\mathrm{w}}}\right)}$$

D_m	N_p
400 nm	94
300 nm	55
200 nm	26
100 nm	7
80 nm	5
60 nm	3

What evidence is required for PCF

- Increase in activated fraction when temperature falls below the homogeneous ice nucleation threshold ✓
- Presence of pores in ice-nucleating particles ✓
- Pore condensation occurring well below water saturation ✓
- Ability of ice to nucleate within very small water volumes ✓
- Ability of ice to grow out of the pores from the vapor phase ✓

What evidence is required for PCF

- Increase in activated fraction when temperature falls below the homogeneous ice nucleation threshold ✓
- Presence of pores in ice-nucleating particles ✓
- Pore condensation occurring well below water saturation ✓
- Ability of ice to nucleate within very small water volumes ✓
- Ability of ice to grow out of the pores from the vapor phase ✓

What evidence is required for deposition nucleation

- Continuous development of activated fraction with temperature ?
- Absence of pores in ice-nucleating particles ?
- Active sites that can template ice from the vapor phase ?
- Active sites that are large enough for ice to grow from the vapor phase on top of them ?

Thank you for your attention!

Questions?